

RESEARCH
ENGINEERING
PRODUCTION



FACILITY FORM 602

<u>N65-25008</u>		_____
<small>(ACCESSION NUMBER)</small>		<small>(THRU)</small>
<u>57</u>	_____	<u>1</u>
<small>(PAGES)</small>	<small>(CODE)</small>	<small>(CATEGORY)</small>
<u>CD 62926</u>	_____	<u>33</u>
<small>(NASA CR OR TMX OR AD NUMBER)</small>		

GPO PRICE \$ _____

OTS PRICE(S) \$ _____

Hard copy (HC) 3.00

Microfiche (MF) .50

EXPERIMENTAL RESULTS FOR
THERMAL IGNITION OF HYDRO-
GEN IN A SUPERSONIC VISCOUS
FLOW

TECHNICAL REPORT NO. 404

by James Dunn

Prepared Under Contract No. NAS8-2686

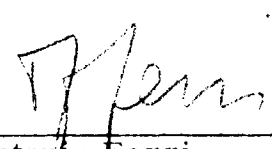
Prepared for

George C. Marshall Space Flight Center
Huntsville, Alabama

Prepared by

General Applied Science Laboratories, Inc.
Merrick & Stewart Avenues
Westbury, L.I., New York

Approved by:



Antonio Ferri
President

December 1963

ABSTRACT

25008

This report contains results of a wind tunnel program to determine ignition characteristics of hydrogen vented from a supersonic or hypersonic launch vehicle. In the test program hydrogen gas was vented into the boundary layer of a two-dimensional Mach 3 flow with 6 psia static pressure and for a range of stagnation temperatures. The experimental results provide a correlation of the onset of combustion with the thermodynamic properties of the flow field and also ignition characteristics associated with surface irregularities or protuberances.

Author

TABLE OF CONTENTS

<u>Section</u>	<u>Title</u>	<u>Page No.</u>
	Abstract	ii
I	Summary	1
II	Introduction	3
III	Description of Apparatus	6
IV	Discussion of Results	12
V	Conclusions	21
VI	Application to Flight Conditions	23
VII	References	23a

LIST OF FIGURES

<u>Figure</u>	<u>Description</u>	<u>Page No.</u>
1	Schematic Representation of Temperature Profiles for Slot Mixing in Vicinity of Splitter Plate	2
2	Wind Tunnel Test Section	25
3	Combustion Preheater	26
4	Wedge for Ignition Studies	27
5	Heat Transfer Gauge	28
6a-b	Heat Transfer Rates Run 65	29
6c-d	" " " "	30
6e-f	" " " "	31
7a-b	Heat Transfer Rates Run 61	32
7c-d	" " " "	33
7e-f	" " " "	34
8a-b	Heat Transfer Rates Run 62	35
8c-d	" " " "	36
8e-f	" " " "	37
9	Top Wall Pressure Distribution Run 65	38
9a	Bottom Wall Pressure Distribution Run 65	39
10	Top Wall Pressure Distribution Run 61	40
10a	Bottom Wall Pressure Distribution Run 61	41
11	Top Wall Pressure Distribution Run 62	42
11a	Bottom Wall Pressure Distribution Run 62	43
12	Ignition Photograph on Wedge	44

<u>Figure</u>	<u>Description</u>	<u>Page No.</u>
13	Ignition Photograph on Disturbance	45
14	Top Wall Pressure Distribution Run 94	46
14a	Bottom Wall Pressure Distribution Run 94	47
15	Mach Number Distribution at Tunnel Exit	48
16	Stagnation Temperature Distribution	49
17	Ignition Delay Time for Hydrogen-Air Reaction	50
18	Reaction Time for Hydrogen-Air Reaction	51
19	Launch Vehicle Trajectory	52
20	Maximum Temperature in Vehicle Boundary Layer for Trajectory in Figure 19	53

EXPERIMENTAL RESULTS FOR THERMAL IGNITION OF
HYDROGEN IN A SUPERSONIC VISCOUS FLOW

James Dunn

I. SUMMARY

Ignition characteristics, pressures and heat transfer have been measured in the hydrogen combustion region downstream of a slot injector exhausting into a Mach 3 flow with nominal static pressure of 6 psia and 10^7 Reynolds number. Three results from this work are listed below.

1. Flow conditions were chosen so that hydrogen dumped from a wall slot would not thermally ignite. A 15° wedge was placed in the flow downstream of the slot and hydrogen was ignited by the increased temperature on the downstream side of the oblique shock produced by the wedge. Thermal ignition occurred if air at a temperature of 1900°R or higher could mix with hydrogen. Ignition delay times are consistent with estimates made with the one dimensional chemical kinetic calculations of Reference 3.
2. Pressure increase in the combustion zone indicate that the reaction was not complete in a distance longer than the theoretical reaction distance. This indicates that the reaction was probably diffusion controlled. Turbulent wall heat transfer rates in the reacting flow were observed to be 30% higher than would be predicted by using heat transfer equations developed for non-reacting flows and taking into account flow field changes associated with the reaction.

3. A series of tests was made with small two dimensional disturbances on the splitter plate upstream of the slot exhaust. Hot gas in the wake of these protuberances ignited hydrogen from the slot in the distances of less than one inch. The disturbance height was less than the boundary layer thickness and the leading edge was cylindrical. This result illustrates that a local disturbance can be a trigger for combustion provided it is blunt enough to produce high temperature air that can mix with hydrogen.

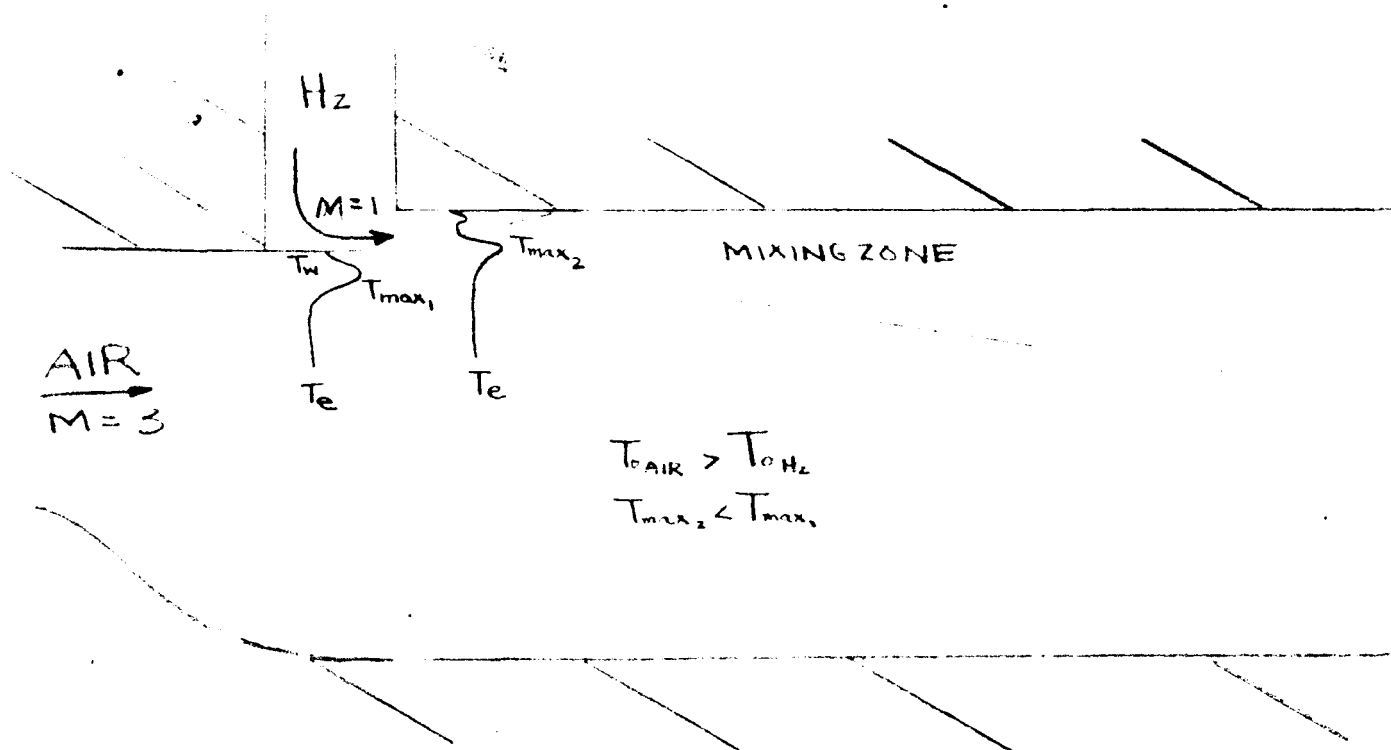


FIGURE 1

Schematic Representation of Temperature Profiles for Slot Mixing
In Vicinity of Splitter Plate

II. INTRODUCTION

During the launch phase of a class of boost vehicles, hydrogen gas is vented from one of the upper stages into the airstream. Combustion of the hydrogen can ensue depending on the conditions of flow and on the venting configuration. If combustion does occur, then significant changes in the heat transfer to the wall of the vehicle and aerodynamic force distributions on the vehicle may result. The analysis of the problem is quite complex as a result of the interaction between the finite rate chemical effects and the shear flow-free stream interactions.

Various aspects of the problem have been considered analytically under the present program, References 1-8. This report presents the results of an experimental study of conditions for ignition of hydrogen in a turbulent boundary layer with particular reference to the effects of small protuberances in the flow. These tests do not simulate the low density conditions of hypersonic launch vehicle flight because of the large ignition delay and combustion distances which apply, but rather attempt to gather information at a more convenient scaling pressure which can be used to correlate with concurrent theoretical studies.

Three significant parameters that determine conditions for thermal ignition of hydrogen dumped from a wall slot are stagnation temperature, local Mach number and wall temperature inasmuch as these quantities set the maximum temperature in the splitter plate boundary layer (Figure 1), that mixes with hydrogen ejected from the slot. In addition to these three parameters, static pressure of the flow affects ignition delay and reaction times of the combustion reaction. The effect of these four quantities on thermal ignition of hydrogen in supersonic flow is reported in References 1, 9, 10 and

11. In these references a temperature for supersonic autoignition of a slot flow is quoted for two different free stream pressures. Reference 9 also contains a significant similitude study for the turbulent mixing of two parallel streams with different densities and velocities.

A conceptual model for autoignition of hydrogen dumped from a wall slot parallel to the external flow is that ignition occurs by hydrogen from the slot mixing with hot gas in the free shear layer that developed from the external splitter plate boundary layer. Provided, of course, the heat content of the wake is large enough to ignite the hydrogen. Ignition for this type of flow is thus controlled largely by the temperature of the gas in the wake that mixes with hydrogen from the slot. A measure of the wake temperature is the maximum temperature of the splitter plate boundary layer at the hydrogen exhaust. The maximum temperature in a boundary layer can be calculated by Crocco's particular energy integral, and is $T_{\max} = T_w + 1/4 \frac{(T_o - T_w)^2}{T_o - T_e}$. The wall (splitter plate) temperature plays an important part in setting the conditions for ignition, especially at low Mach numbers.

The scaling laws for the mixing of two parallel turbulent compressible flows has been reported in Reference 10 with the important result that the spread of the mixing zone depends on the ratio $\frac{(\rho u)_j}{(\rho u)_e}$, and is independent of free stream velocity per se. Thus ignition characteristics can be studied at an arbitrary free stream velocity and the parameters to simulate are the temperature in the splitter plate wake, the ratio $\frac{(\rho u)_j}{(\rho u)_e}$ and the static pressure of the flow. The ignition delay and energy release times for the combustion of hydrogen with air are pressure dependent as shown by the chemical kinetics calculations of Reference 11.

In References 9 and 10 supersonic flow ignition temperatures are reported for hydrogen air reaction at pressures of 15 psia and 6 psia. These tests were performed for two values of the parameter $\frac{(\rho u)_j}{(\rho u)_e}$. Turbulent mixing data for a range of $\frac{(\rho u)_j}{(\rho u)_e}$ (without combustion) will be the subject of a forthcoming GASL report. Also given in Reference 10 are heat transfer rates with and without combustion.

III. DESCRIPTION OF APPARATUS

1. Wind Tunnel Test Section

The tests were conducted in a combustion heated blow-down wind tunnel that exhausts to the atmosphere. The test section was two dimensional with a contoured half nozzle and exit size of $1\frac{3}{4} \times 3\frac{1}{2}$ inches. The test section is shown schematically in Figure 1 and in more detail in Figure 2. The test section had four windows for taking luminosity photographs, shadow-graphs or motion pictures. Static pressures were measured along the top, bottom and side walls. Heat transfer rates were measured on the top wall with thermocouple gauges. Pitot pressures were measured at the tunnel exit to ascertain that the flow was supersonic after combustion and total temperature profiles were measured ahead of the flame zone to establish the homogeneity of the flow. A typical test duration for this program was fifteen seconds.

2. Combustion Heater

The GASL combustion heater burns a mixture of hydrogen and oxygen in air to produce products of combustion with an oxygen mass fraction equal to the oxygen content of uncontaminated air. This mixture of H_2O , N_2 and O_2 is called vitiated air and typical mass fractions ($2500^\circ R$) would be 0.23 oxygen, 0.10 water and 0.67 nitrogen as compared to uncontaminated air with 0.23 oxygen and 0.77 nitrogen. In the expanded flow of the test section the water and nitrogen will be essentially inert dilutents and it is believed will have no significant effect on the chemistry of the problem considered in this report.

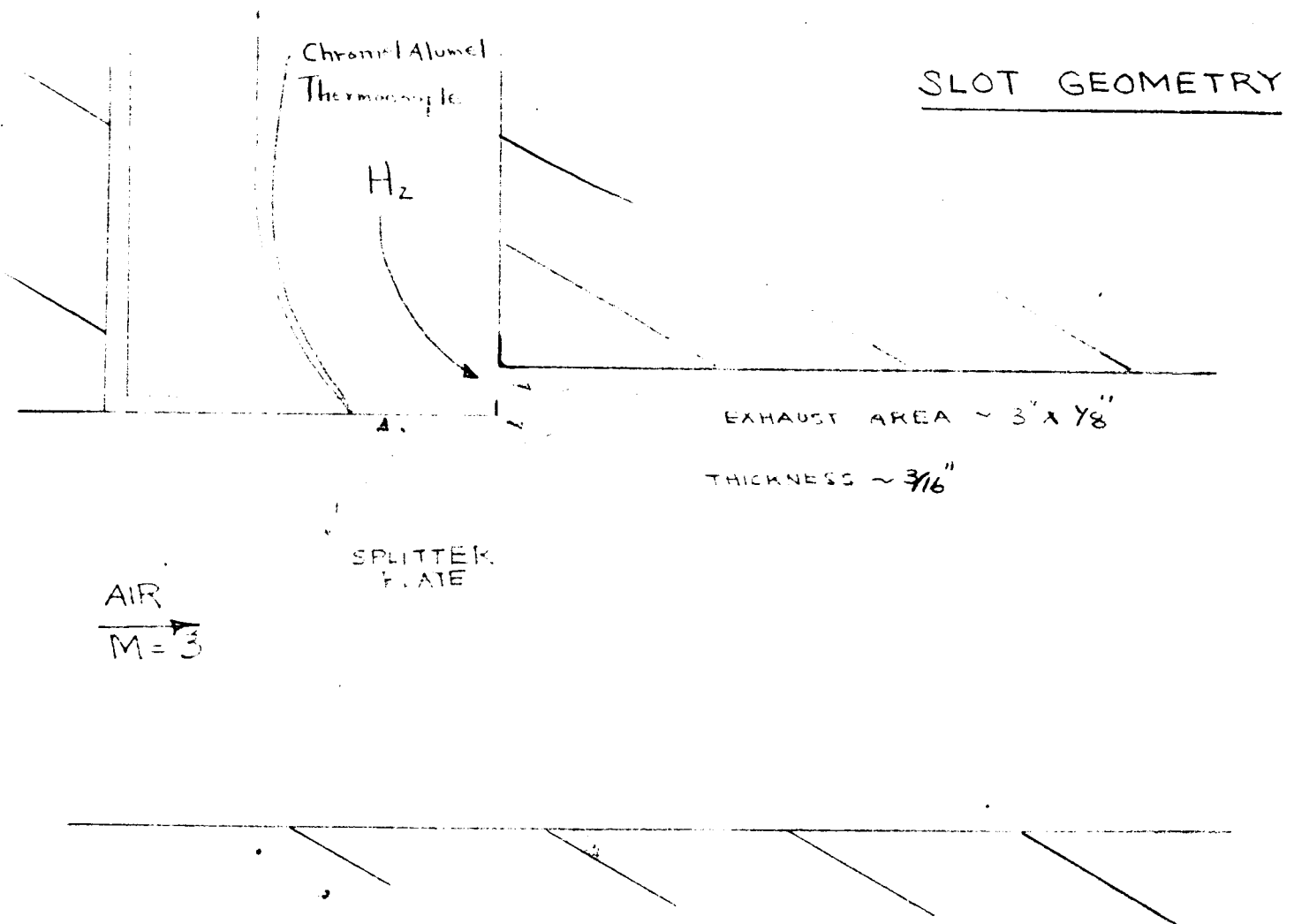
The portions of hydrogen and oxygen added to the air stream are calculated to produce a specific temperature of the products and the chemical composition discussed above. The oxygen and hydrogen are introduced into the air in preset quantities and the flow rates are controlled by commercial regulators. Air for the burner is compressed and stored in a bank of tanks at pressures up to 2000 psi. The combustion gases are stored in manifolds of commercial gas bottles. The flow rates of oxygen, air and hydrogen are monitored with venturis and the pressures are measured with transducers.

Hydrogen and oxygen are injected into a plenum chamber through a multi-holed ring injector to promote thorough mixing with the air flow. The mixture is ignited with a 15,000 volt spark and the products of combustion are confined in a 7" diameter steel tube that is 5' long. The pressure of the products is measured in the subsonic flow ahead of the throat and the total temperature is measured with two platinum-rhodium thermocouples. The vitiated air passes from the combustion tube through the two-dimensional throat and then into the test section. Figure 3 shows a cross-sectional view of the combustion chamber.

3. Hydrogen Wall Slot

Hydrogen was dumped into the test section through a wall slot as shown in Figure 1. The wall slot was located in the fully expanded section of the wind tunnel, and was 3" wide by 1/8" high. The nozzle plenum pressure was set at 12 psia nominal to match static pressure of the slot flow with static pressure of the free stream. For all tests the total temperature of the hydrogen was approximately 530°R. The plate that forms the boundary between the air flow and hydrogen flow is called the splitter plate in this report. The splitter plate used in these tests was approximately 3/16" thick

and had a fast response chromel-alumel thermocouple heliarced to the surface. The detailed shape of the slot is shown in the cross sectional sketch below.



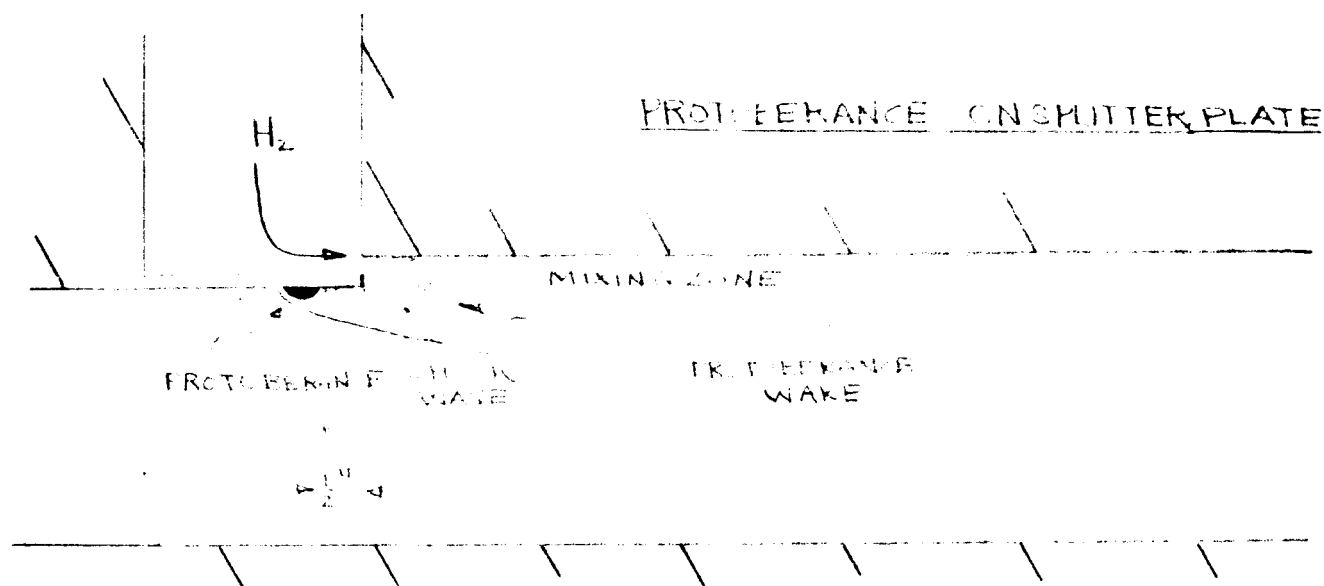
The H_2 mass flow rate for the tests in this series was .015 lb/sec or an equivalence ratio of 0.2.

4. Wedge for Combustion Studies

A 15° half angle wedge was placed on the top wall of test section for the series of wedge burning tests. Recall that the top wall of the tunnel is straight and the hydrogen slot is on this wall whereas the bottom wall is contoured to obtain the Mach 3 flow. The wedge was located $9\frac{1}{4}$ " downstream of the slot exit or 74 slot heights downstream. The wedge was 0.45" high by $2\frac{1}{4}$ " wide and fillers were used to streamline the corners and thereby reduce the disturbance in the corner. The wedge did not span the test section because the area reduction of a $3\frac{1}{2}$ " wide wedge was large enough to choke the wind tunnel. The wedge was made symmetrical in the streamwise direction rather than as a plateau to prevent thermal choking of the tunnel due to heat release in the combustion zone. A plateau type wedge was built and used for one test series but the tunnel choked after combustion. Pressure ports were built into the upstream and downstream side of the wedge.

5. Disturbances on Splitter Plate

A half-cylindrical stainless steel rod was welded to the splitter plate to assess the effect of local protuberances on ignition characteristics. Two different size rods were used, one with a $1/16$ " radius and the second with a $3/16$ " radius. The rod length was $3\frac{1}{2}$ " (test section width) and each was heliarced to the splitter plate on the air side. The rod radii were chosen to be less than the boundary layer thickness which was roughly $1/4$ ". The rods were axially located one half inch upstream of the hydrogen slot exhaust. The following sketch shows the protuberance location:



6. Instrumentation

a) Pressure

Pressures were measured with strain gauge and variable reluctance transducers. The outputs were recorded on high speed oscillographs which ordinarily were operated at 4 " per second. Transducers were calibrated daily. A Scanni-valve was used to multiplex a number of the static pressures on the wall.

b) Temperature

Temperatures were measured with either platinum-rhodium or chromel-alumel thermocouples. The outputs were recorded on an oscillograph or alternately on a mechanical recorder.

c) Heat Transfer

Transient heat transfer rates were obtained by measuring the surface temperature rise of a semi-infinite slab. The measured surface temperature was converted to time varying heat flux by a straight forward numerical integration of the heat-transfer equation. The details of the solution

are covered adequately in References 12 and 13. The heat transfer gauge is shown in Figure 5.

d) Pitot Tube and Total Temperature Rakes

A three prong total pressure rake was used at the tunnel exit to ascertain that the flow was supersonic after combustion occurred. The rake was pulsed into the flow by an air cylinder and remained in the flow for $1/3$ second, nominal.

A four prong stagnation temperature rake was installed below the test section and could be inserted in the flow for durations of $1/4$ second or more. Platinum-rhodium thermocouples were used to measure vertical distributions of total temperature and thereby ascertain that no sizable temperature gradients existed in the flow field.

IV. DISCUSSION OF RESULTS

The principal work reported here is the condition for autoignition when hydrogen from a wall slot flows through an oblique shock wave such as would be produced by a launch vehicle transition section. The tests were performed for temperature conditions (T_o , T_e , T_w) such that the splitter plate wake was not hot enough to ignite hydrogen from the slot. The tests were made in the Mach 3, two-dimensional wind tunnel described in Section II. A 15° wedge was placed on the upper wall of the wind tunnel and hydrogen was dumped from the slot which was located 74 slot heights upstream of the wedge. One test was made with stagnation temperature low enough so that the hydrogen did not burn either on the splitter plate or on the wedge. Two tests were made with a stagnation temperature high enough that the hydrogen ignited when it crossed the shock.

The temperature conditions for the tests are listed in Table 1.

TABLE 1

Number	Stagnation Temp °R	Splitter Plate temp. at time of H ₂ injection °R	Cal. Max. Temp. in splitter Plate boundary layer * °R	Temp. of Col. 2 after pass. . thru Shock °R	Results
61	2600	1200	1500	1900	Ignited on Wedge
62	2700	1150	1500	1900	" " "
65	2200	1050	1250	1600	No Ignition

* $\gamma = 1.33$

Note that hydrogen from the slot did not ignite when mixed with air from the splitter plate boundary layer at a calculated temperature of 1500°R or less. Also given in Table 1 is a calculated temperature increase on the downstream side of the oblique shock wave.

If the hot gas from the splitter plate boundary layer had crossed the shock wave without mixing with hydrogen or cooler air, then a maximum gas temperature of 1900°R downstream of the shock would have ignited the hydrogen as indicated in Column 5 of Table 1. The concept of supersonic autoignition occurring if hydrogen is mixed with air at a certain temperature is, of course, a gross oversimplification since ignition and flame propagation are controlled by the complete heat balance for the reacting gas. In addition, the hydrogen was heated by the hot upper wall. Nevertheless to an engineering approximation, it would appear from these results that if hydrogen from a wall slot is mixed with air at a temperature some place between 1600°R and 1900°R that autoignition can be expected ($p=6$ psia). This result is in agreement with the widely used value of 1800°R for autoignition of hydrogen-air mixtures.

A. Pressure and Heat Transfer Results

Figures 9, 10 and 11 show static pressures measured in the test section for the 3 runs in Table 1. Figures 9 and 9a show the top and bottom wall static pressures for run 65. (No Ignition). Note that no pressure rise was measured ahead of the wedge, which indicates that the boundary layer did not separate. If the empirical separation data in Reference 7 is employed the plateau pressure for wedge type separation would be 15 psi, which was not observed. Additionally, the separation correlations of Reference 6 indicate that for air flow at Mach 3 and 10^7 Reynolds number a $\Delta P/q$ of 0.35 is

required to separate the turbulent boundary layer approaching a wedge. The 15° wedge pressure coefficient is 0.29 at Mach 3, which further suggests that the boundary layer did not separate in the corner. The difference in pressure level between the measurements before slot injection and after injection were due to a slight drift in tunnel stagnation pressure. The low pressure region on the bottom wall downstream of the slot before injection is caused by the expansion fan originating at the splitter plate lip. Downstream of the wedge the oblique shock wave reflects from the bottom wall and hits the top wall again, causing a high pressure region on the top wall.

Figure 6a through 6e show Run 65 - heat transfer rates on the top wall. The duration of hydrogen injection is indicated on each figure. The location of the gauges is indicated in Figure 9 in relation to the slot and wedge. Figure 6 also contains the calculated flat plate heat transfer rate.

$$q = \frac{.0296}{Pr^{2/3}} \frac{(\rho_e u_e) (h_r - h_w)}{(Re_x)^{.2}} \left[\left(\frac{\rho_e}{\rho^*} \right)^{.8} \left(\frac{\mu^*}{\mu_e} \right)^{.2} \right] \quad (1)$$

This is the turbulent heat transfer rate calculated by Reynold's analogy using the constant-property Blasius incompressible skin friction relation and Eckert's reference enthalpy factor for compressibility. (Reference 16). Agreement between calculated and measured heat flux is within 12% before hydrogen injection except for gauge 3. The discrepancy for gauge 3 is felt to be an experimental error, rather than low heat flux in a separated region on the basis of the pressure measurements and previous discussion. The steady decrease of heat flux before injection was caused by the rising surface temperature. For instance, the wall temperature rose from $900^\circ R$

to 1100°R for gauge 1 in the time interval of five to nine seconds. Gauges 1 and 2 show the decrease in heat flux when the cold ($T_0=540^{\circ}\text{R}$) hydrogen is injected into the test section. Gauge 3 does not change during hydrogen injection indicating that the hydrogen was at least partially mixed with the air at this location, i.e., 66 slot heights downstream. Gauges 4 and 5 were downstream of the wedge and yielded no significant information for the no-burning test. The tail-off at the end of each heat flux trace represents the tunnel shut down. No attempt was made to explain the 12% difference between measured and calculated heat flux since the measurements were made primarily to compare heat transfer with and without combustion and 12% may be considered reasonable engineering agreement.

Figure 10 and 10a give pressure distributions for Run 61, in which the hydrogen burned downstream of the wedge. Note that the pressure level behind the wedge increased from seven psia to 14 psia, due to the heat release in this region. The distance from the onset of combustion to the end of the tunnel was about ten inches and combustion was not complete in this distance as indicated by comparing the observed pressure rise with a one dimensional estimate. Despite this fact, a simple one-dimensional calculation of changes in flow properties can be made using the measured static pressures, as an indication of the heat release. The dynamic and thermodynamic properties obtained from the one-dimensional calculation can then be used with the flat plate turbulent heat transfer equation to calculate a new heat flux, ignoring any combustion-induced changes in the mechanism of heat transfer. This type of calculation was made for Run 61. Table 2 contains a summary of these results.

TABLE 2

Heat Flux Calculation for Runs 61 & 62 (All heat flux in $\frac{\text{BTU}}{\text{ft}^2 \text{ sec}}$)								
Run No.	Gauge No.	\dot{q} theor no. comb.	\dot{q} theor with comb.	$\frac{\dot{q} \text{ comb.}}{\dot{q} \text{ no comb. theor.}}$	\dot{q} meas. no. comb.	\dot{q} meas. with comb.	$\frac{\dot{q} \text{ comb.}}{\dot{q} \text{ no comb. meas.}}$	Ratio meas. calcu.
I	II	III	IV	IV \div III	VI	VII	VII \div VI	IX
61	5	43	70	1.63	38	77	2.0	1.23
61	6	40	76	1.91	43	100	2.3	1.21
62	5	45	69	1.54	48	83	1.7	1.10
62	6	47	74	1.56	55	110	2.0	1.29

The individual curves of heat transfer rates for Run 61 are given in Figure 7a-7f. No qualitative differences from the no burning test are evident except for gauges 5 and 6 which are in the combustion region downstream of the wedge. Increases in heat transfer rates of 2.0 and 2.3 are observed for gauges 5 and 6. These ratios are not felt to be representative of heat transfer increases that would occur in the external flow on a vehicle since these results are for flow in a constant area channel; however, a different type of calculation can be made for an external application. It appears from the calculation and results in Table 2 that turbulent heat transfer in the combustion region can be calculated to within 30% by using the flow properties evaluated in the burning gas and the heat flux equation developed from non-reacting data. To calculate the heat flux in an external flow with hydrogen combustion the flow field with combustion would have to be calculated and then Equation (1) would be used to

estimate the heat transfer rate and subsequently increased by a factor of 1.3. Figure 12 is a luminosity photograph taken during the burning portion of test 61. This picture indicates that the flame zone starts immediately behind the wedge apex and that hydrogen was still concentrated on the top wall after the compression and subsequent re-expansion around the wedge. Also given in Figure 12 is a schematic aid for interpreting the luminosity photo.

Run 62 was an additional test with combustion on the downstream side of the wedge. The pressure distributions for this run are given in Figure 11 and 11a. No qualitative differences exist between the pressures in this run and run 61 which was previously discussed. Figures 8a to 8e show heat transfer rates for test 61. Once again, the wall cooling is observed near the slot exit and heat transfer increases occur in the combustion region behind the wedge. Gauges 5 and 6 indicate gross heat flux increases of 1.7 and 2.0 during combustion. These ratios are compared to the calculated ratios in Table 2. The agreement of the theoretical with experimental ratios of heat flux with combustion to heat flux without combustion is once again within 30%.

B. Ignition Delay Time

In previous work at GASL (Ref. 11) curve fits to calculations for ignition delay and reactions times were developed for the combustion of hydrogen in air. It is difficult to interpret experimental data in terms of theoretically defined ignition delay times; however, in Ref. 11 a measure of experimental ignition delay time was taken as the length at which visible radiation was first observed on a long exposure photograph divided by a characteristic flow velocity. In this sense Figure 12 can be used to estimate a distance from the beginning of the observed flame back to the shock wave and a characteristic velocity can be taken as the inviscid air velocity on the wedge. This calculation

gives $\tau_{ID} = \frac{1.6 \text{ inches}}{4200 \text{ fps } 12 \text{ inch/ft.}} = 32 \mu \text{ sec.}$ If the empirical relation

$$\tau_{ID} = \frac{8 \times 10^{-3}}{p} \exp \frac{9600}{T} \text{ is used to calculate an ignition delay time, then}$$

$\tau_{ID} = 57 \mu \text{ sec.}$ This was calculated using the measured pressure on the wedge and the "unmixed" maximum splitter plate boundary layer temperature downstream of the shock wave. This is considered a reasonable agreement between theory and experiment. It is not possible to compare theoretical reaction times from Reference 11 with any characteristic distance of the flow because the flow was not reaction rate controlled. That is, the hydrogen did not completely burn in the 10 inches from the wedge to the tunnel exit whereas the theoretical reaction distance is $L_R = u_{\infty} \tau_R = 4900 \text{ fps } \frac{105}{p} \exp \frac{-1.12T}{1000} = 5'$. This is the distance in which the reaction would have reached equilibrium if the hydrogen and air had been premixed when ignition occurred, which of course, is not indicated by the theoretical calculation of reaction time.

A rough measure of how much of the hydrogen had reacted at the tunnel exit can be obtained from the static pressure rise downstream of the wedge. The static pressure rise of approximately 2.0 (Run 61) yields a one-dimensional simple To change of about 1.24. Using the tunnel mass flow rate of 2.6 lb/sec this yields a heat release of 500 BTU as compared to a heat of $Q = \dot{m} \Delta H = (.015 \text{ lb/sec.})(55000 \text{ BTU/lb}) = 800 \text{ BTU}$ for complete combustion. These calculations were made to demonstrate that the measured heat transfer rates were taken in a diffusion controlled reacting flow and that no conclusions can be made from this data about heat flux for downstream on a vehicle after the reaction has reached equilibrium.

A total pressure survey was made at the tunnel exit to be sure that combustion was not choking the tunnel. Figure 15 shows the Mach number

distribution calculated from this run. Note that the Mach number is lower at the top where hydrogen is burning than in the non-reacting gas at the bottom wall. An additional run was made with a total temperature rake to check the temperature distribution in the test section. Figure 17 is the measured profile 2 inches downstream of the slot exhaust. The test section measured temperatures are 150° lower than the 2900°R measured in the subsonic plenum chamber but no recovery factor was applied to the probes in the supersonic test section. The profiles show that the vitiated air entering the nozzle was mixed enough to provide a uniform temperature distribution.

C. Ignition by Two-Dimensional Disturbance on Splitter Plate Lip

A series of tests was made with a disturbance on the free stream side of the splitter plate as shown in the sketch on Page 9. The purpose of this test series was to determine if hydrogen can be ignited by a local disturbance that serves as a source of hot gas. Recall from the description in Section II that the disturbance was half of a circular cylinder and spanned the test section. One cylinder was $1/16''$ high and the second was $3/16''$. Hydrogen from the slot was ignited within one inch of the exhaust by either rod. The tunnel was run at conditions (see Table 5 for T_o , T_e , T_w) such that the slot hydrogen would not have burned any place in the tunnel if the disturbance had not been on the splitter plate. Note that the calculated maximum splitter plate boundary layer temperature was in all cases lower than 1600°R and that results in Section B indicate that hydrogen from the slot would not have been ignited for a temperature this low. Reference 10 also contains some pertinent data on this topic. Figure 13 is a luminosity photograph of hydrogen

combustion triggered by the two different disturbances. As an aid to interpreting these photographs the reader is referred again to the sketch on Page 9.

TABLE 3

Run No.	Disturbance	T_o °R	T_w °R	T_{max} °R	Results
88	3/16	2700	1350	1600	burned at splitter plate lip
90	3/16	2400	1250	1450	" " " "
91	1/16	2600	1350	1600	" " " "
93	1/16	2800	1150	1550	" " " "
95	1/16	2900	1050	1500	" " " "

The hydrogen ignition and short ignition delay distance (approximately one inch) is attributed to the high temperature in the viscous wake behind the blunt cylinder and perhaps also to enhanced mixing of the hydrogen and air in the presence of the large free shear region shed from the rod. Static pressures were measured on the tunnel wall downstream of the slot. This data is given in Figures 14 and 14a and is presented mainly to demonstrate conclusively that combustion occurred in the presence of the disturbance. The boundary layer thickness on the splitter plate was estimated to be about one quarter inch at the location of the disturbance and the displacement thickness was about 0.1". Both disturbances were within the estimated boundary layer.

V.. CONCLUSIONS

1. Slot flow autoignition of hydrogen in air can be expected if the maximum temperature of the splitter plate boundary layer is 1900°R or higher. The temperature for autoignition is probably below 1900°R but is definitely above 1600°R . This applies to a flow with static pressure of 6 psia and with a splitter plate thickness at least $1/8$ ". The principal effect of static pressure will be to change the ignition delay and reaction times (lengths) as shown by Figures 17 and 18.
2. Thermal ignition of unburned hydrogen from a slot that is compressed by passing through a shock can be expected if the "unmixed" maximum splitter plate boundary layer temperature is raised to 1900°R by the shock. (The qualifying comments in Item 1 apply here also.) Alternatively, if the maximum temperature in a hydrogen air boundary layer is raised to 1900°R by passing through a shock thermal ignition can be expected.
3. A blunt disturbance ahead of the slot exhaust with a height equal to or greater than the boundary layer displacement thickness can generate enough hot gas to significantly alter the ignition characteristic of the slot flow. It is difficult to make a quantitative estimate of the temperature conditions for which a protuberance will ignite the slot hydrogen. However, if a maximum temperature can be assigned to the protuberance wake at the slot exhaust then 1900°R could tentatively be taken as an ignition temperature (at 6 psia).
4. The theoretical ignition delay curve of Reference 11 (also Figure 17) appears to be in reasonable quantitative agreement with results from these tests and previous GASL work.

5. Heat transfer increases of 1.7 to 2.3 were measured during combustion in a constant area channel. Turbulent wall heat transfer rates in the reacting flow were observed to be 30% higher than would be predicted by using heat transfer relations developed for non-reacting flow and using flow properties of the burning gas.

VI. APPLICATION TO FLIGHT CONDITIONS

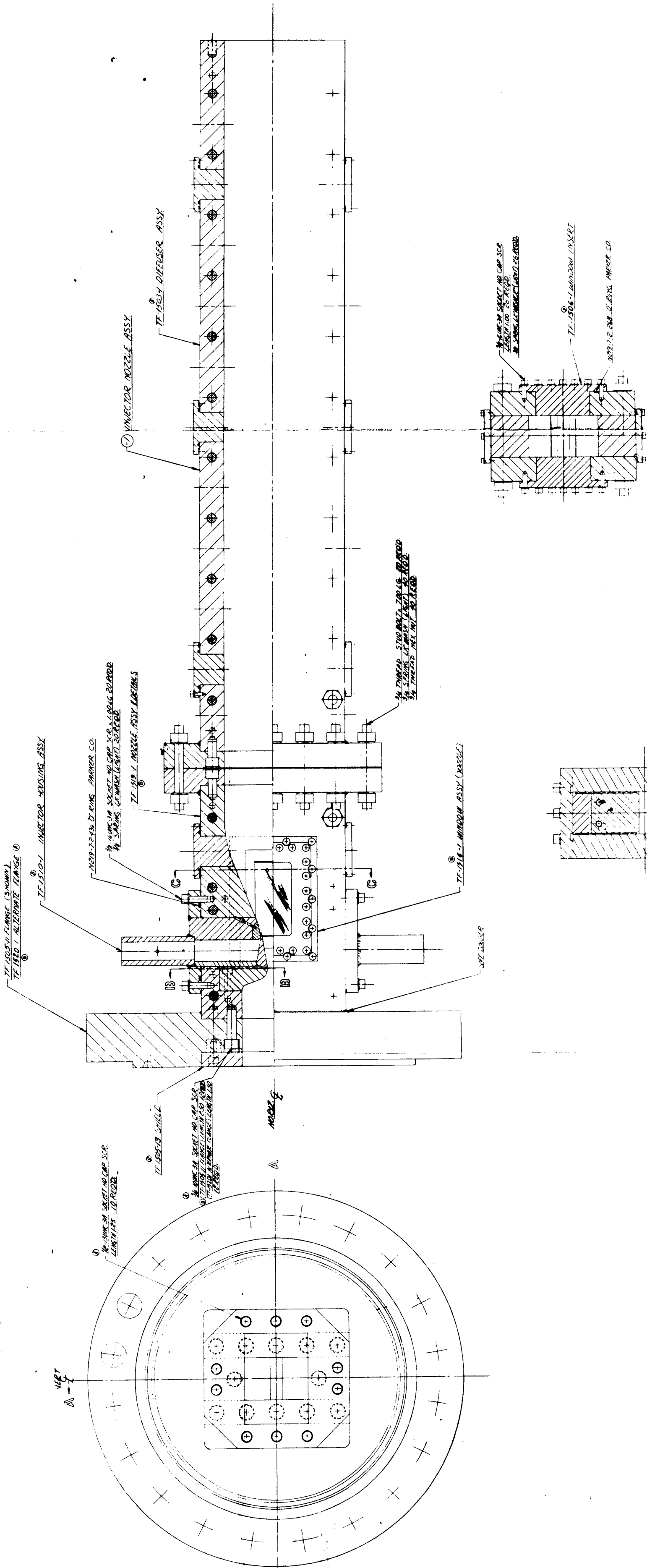
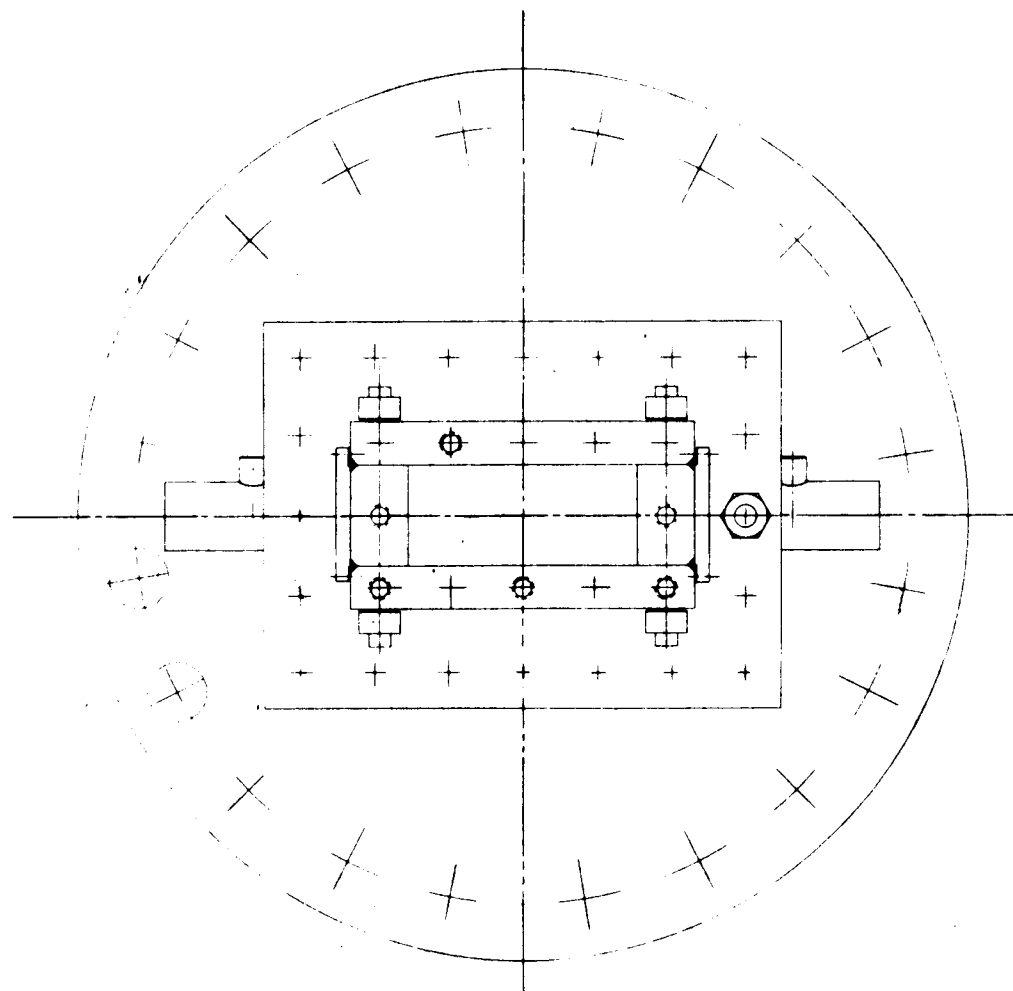
A sample calculation for thermal ignition of hydrogen dumped from a wall slot was made for the typical launch vehicle trajectory shown in Figure 19. Figure 20 shows the results of this calculation and indicates that (based on the results of this program) thermal ignition can be expected at altitudes above 130,000 feet. For ignition delay and reaction lengths Figure 17 and 18 can be used along with the local velocity of the flow. Ignition delay lengths may of course be longer than the booster at high altitudes as has been previously reported in Reference 1.

REFERENCES

1. Libby, P.A., Pergament, H. S., Taub, P. "Engineering Estimates of Flow Lengths Associated With the Combustion of Hydrogen-Air Mixtures During a Launch Trajectory, GASL Technical Report No. 330, December 1962.
2. Rosenbaum, H., "Axisymmetric Laminar and Turbulent Jets of Hydrogen with Simple Chemistry, GASL Technical Report No. 331, January 1963.
3. Taub, P.A., "Slot Injection of Reactive Gases in Laminar Flow with Application to Hydrogen Dumping", GASL Technical Report No. 332, January 1963.
4. Edelman, R., Rosenbaum, H., Slutsky, S., "Generalized Viscous Multicomponent-Multiphase Flow with Application to Laminar and Turbulent Jets of Hydrogen", GASL Technical Report 349, June 1963.
5. Edelman, R., and Rosenbaum, H., "Finite Rate Evaporation of Cryogenic Hydrogen in Two-Phase Air", GASL Technical Report No. 367, September 1963.
6. Rosenbaum, H., "Induced Pressure Forces Due to Hydrogen Dumping" GASL Technical Report No. 365, July 1963.
7. Edelman, R., and Libby, P.A., "A Preliminary Analysis of a Reacting Boundary Layer with Coupled Pressure Interaction", GASL Technical Report No. 377, November 1963.
8. Libby, P.A., Rosenbaum, H., and Slutsky, S., "The Laminar Boundary Layer in Hydrogen-Air Mixtures with Finite Rate Chemistry", GASL Technical Report No. 385, November 1963.
9. Schetz, J.A., "Diffusion and Combustion of Hydrogen in Air at Supersonic Speeds" (U) Report Confidential, GASL Technical Report No. 319, November 1962.
10. Schetz, J. A., Dunn, J. E., "Thermal Ignition of Slot Injected Hydrogen for Low Free Stream Temperature and Pressure "(U) Report Confidential, GASL Technical Memo No. 92, November 1963.
11. Pergament, H. S., "A Theoretical Analysis of Non-Equilibrium Hydrogen-Air Reactions in Flow Systems", AIAA-ASME Hypersonic Ramjet Conference, April 1963, Paper 63113
12. Cresci, R. J., and Libby, P.A., "Some Heat Conduction Solutions Involved in Transient Heat Transfer Measurements", WADC Technical Note 57-236, ASTIA AD130800, September 1957.

13. Bello, B.A., "Control Data 160-A SICOM Program for Computation of Aerodynamic Heat Transfer Rate for any Measured Surface Temperature History", GASL Internal Document. (Available on Request).
- > 14. Kaplan, M.A., and Estes, T.J., "High Speed Boundary Layer Separation in a Compression Corner", General Electric Missile and Space Vehicle Department, Thermodynamics Fundamental Memorandum, TFM-HTT-8151-001.
15. Pallone, A., and Erdos, J., "Shock Boundary Layer Interaction and Flow Separation", AVCO Research and Development, RAD TR 61-23.
16. Eckert, E.R.G., "Engineering Relations for Heat Transfer in High Velocity Laminar and Turbulent Boundary Layer Flow Over Surfaces with Constant Pressure and Temperature", ASME Paper No. 55-A31, November 1955.

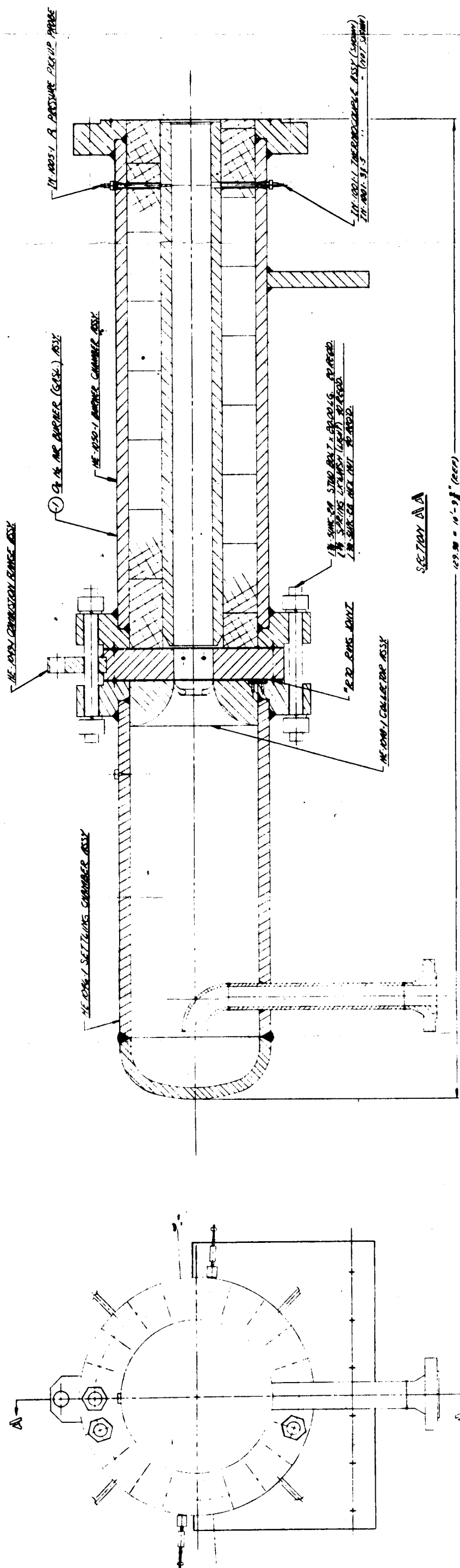
FIGURE 2



1. PORT-1000
 2. PORT-1000
 3. PORT-1000
 4. PORT-1000
 5. PORT-1000
 6. PORT-1000
 7. PORT-1000
 8. PORT-1000
 9. PORT-1000
 10. PORT-1000
 11. PORT-1000
 12. PORT-1000
 13. PORT-1000
 14. PORT-1000
 15. PORT-1000
 16. PORT-1000
 17. PORT-1000
 18. PORT-1000
 19. PORT-1000
 20. PORT-1000
 21. PORT-1000
 22. PORT-1000
 23. PORT-1000
 24. PORT-1000
 25. PORT-1000
 26. PORT-1000
 27. PORT-1000
 28. PORT-1000
 29. PORT-1000
 30. PORT-1000
 31. PORT-1000
 32. PORT-1000
 33. PORT-1000
 34. PORT-1000
 35. PORT-1000
 36. PORT-1000
 37. PORT-1000
 38. PORT-1000
 39. PORT-1000
 40. PORT-1000
 41. PORT-1000
 42. PORT-1000
 43. PORT-1000
 44. PORT-1000
 45. PORT-1000
 46. PORT-1000
 47. PORT-1000
 48. PORT-1000
 49. PORT-1000
 50. PORT-1000
 51. PORT-1000
 52. PORT-1000
 53. PORT-1000
 54. PORT-1000
 55. PORT-1000
 56. PORT-1000
 57. PORT-1000
 58. PORT-1000
 59. PORT-1000
 60. PORT-1000
 61. PORT-1000
 62. PORT-1000
 63. PORT-1000
 64. PORT-1000
 65. PORT-1000
 66. PORT-1000
 67. PORT-1000
 68. PORT-1000
 69. PORT-1000
 70. PORT-1000
 71. PORT-1000
 72. PORT-1000
 73. PORT-1000
 74. PORT-1000
 75. PORT-1000
 76. PORT-1000
 77. PORT-1000
 78. PORT-1000
 79. PORT-1000
 80. PORT-1000
 81. PORT-1000
 82. PORT-1000
 83. PORT-1000
 84. PORT-1000
 85. PORT-1000
 86. PORT-1000
 87. PORT-1000
 88. PORT-1000
 89. PORT-1000
 90. PORT-1000
 91. PORT-1000
 92. PORT-1000
 93. PORT-1000
 94. PORT-1000
 95. PORT-1000
 96. PORT-1000
 97. PORT-1000
 98. PORT-1000
 99. PORT-1000
 100. PORT-1000

8
COMBUSTION TEST
ASSY
100-1-1504

8
COMBUSTION TEST
ASSY
100-1-1504



200 mg/kg
 100 mg/kg
 50 mg/kg
 25 mg/kg
 12.5 mg/kg
 6.25 mg/kg
 3.125 mg/kg
 1.5625 mg/kg
 0.78125 mg/kg
 0.390625 mg/kg
 0.1953125 mg/kg
 0.09765625 mg/kg
 0.048828125 mg/kg
 0.0244140625 mg/kg
 0.01220703125 mg/kg
 0.006103515625 mg/kg
 0.0030517578125 mg/kg
 0.00152587890625 mg/kg
 0.000762939453125 mg/kg
 0.0003814697265625 mg/kg
 0.00019073486328125 mg/kg
 0.000095367431640625 mg/kg
 0.0000476837158203125 mg/kg
 0.00002384185791015625 mg/kg
 0.000011920928955078125 mg/kg
 0.0000059604644775390625 mg/kg
 0.00000298023223876953125 mg/kg
 0.000001490116119384765625 mg/kg
 0.0000007450580596923828125 mg/kg
 0.00000037252902984619140625 mg/kg
 0.000000186264514923095703125 mg/kg
 0.0000000931322574615478515625 mg/kg
 0.00000004656612873077392578125 mg/kg
 0.000000023283064365386962890625 mg/kg
 0.0000000116415321826934814453125 mg/kg
 0.00000000582076609134674072265625 mg/kg
 0.000000002910383045673370361328125 mg/kg
 0.0000000014551915228366851806640625 mg/kg
 0.00000000072759576141834259033203125 mg/kg
 0.000000000363797880709171295166015625 mg/kg
 0.0000000001818989403545856475830078125 mg/kg
 0.00000000009094947017729282379150390625 mg/kg
 0.000000000045474735088646411895751953125 mg/kg
 0.0000000000227373675443232059478759765625 mg/kg
 0.00000000001136868377216160297393798828125 mg/kg
 0.000000000005684341886080801486968994140625 mg/kg
 0.0000000000028421709430404007434844970703125 mg/kg
 0.00000000000142108547152020037174224853515625 mg/kg
 0.000000000000710542735760100185871124267578125 mg/kg
 0.0000000000003552713678800500929355621337890625 mg/kg
 0.00000000000017763568394002504646778106689453125 mg/kg
 0.000000000000088817841970012523233890533447265625 mg/kg
 0.0000000000000444089209850062616169452667236328125 mg/kg
 0.00000000000002220446049250313080847263336181640625 mg/kg
 0.000000000000011102230246251565404236316680908203125 mg/kg
 0.0000000000000055511151231257827021181583340541015625 mg/kg
 0.00000000000000277555756156289135105907916702705078125 mg/kg
 0.000000000000001387778780781445675529539583513525390625 mg/kg
 0.0000000000000006938893903907228377647697917567626953125 mg/kg
 0.00000000000000034694469519536141888238489587838134765625 mg/kg
 0.000000000000000173472347597680709441192447939190673828125 mg/kg
 0.0000000000000000867361737988403547205962239695953369140625 mg/kg
 0.00000000000000004336808689942017736029811198479766845703125 mg/kg
 0.000000000000000021684043449710088680149055992398834228515625 mg/kg
 0.0000000000000000108420217248550443400745279961994171142578125 mg/kg
 0.000000000000000005421010862427522170037263998099708557145625 mg/kg
 0.0000000000000000027105054312137610850186319990498542783728125 mg/kg
 0.00000000000000000135525271560688054250931599952492713918640625 mg/kg
 0.000000000000000000677626357803440271254657999762463569593203125 mg/kg
 0.0000000000000000003388131789017201356273289998812317847966015625 mg/kg
 0.00000000000000000016940658945086006781366449994061589239830078125 mg/kg
 0.000000000000000000084703294725430033906832249970307946199150390625 mg/kg
 0.0000000000000000000423516473627150169534161249851539730995751953125 mg/kg
 0.00000000000000000002117582368135750847670806249257698654978759765625 mg/kg
 0.000000000000000000010587911840678754238354031246288493274893798828125 mg/kg
 0.0000000000000000000052939559203393771191770156231442466374468994140625 mg/kg
 0.00000000000000000000264697796016968855958850781172123331872344970703125 mg/kg
 0.000000000000000000001323488980084844279794253905860616659361724853515625 mg/kg
 0.0000000000000000000006617444900424221398971269529303083296808624267578125 mg/kg
 0.00000000000000000000033087224502121106994856347646515416484043121337890625 mg/kg
 0.000000000000000000000165436122510605534974281738232577082420215606689453125 mg/kg
 0.0000000000000000000000827180612553027674871408691162885412101078033447265625 mg/kg
 0.00000000000000000000004135903062765138374357043455814427060505390167236328125 mg/kg
 0.000000000000000000000020679515313825691871785217279072135302526950836181640625 mg/kg
 0.0000000000000000000000103397576569128459358926086395360676512634754180908203125 mg/kg
 0.0000000000000000000000051698788284564229

DATE: 06-17-95 APPROVED BY: [Signature] 105-1
[Signature] ASST.
[Signature] 1095

WEDGE
FOR HYDROGEN BURNING TEST

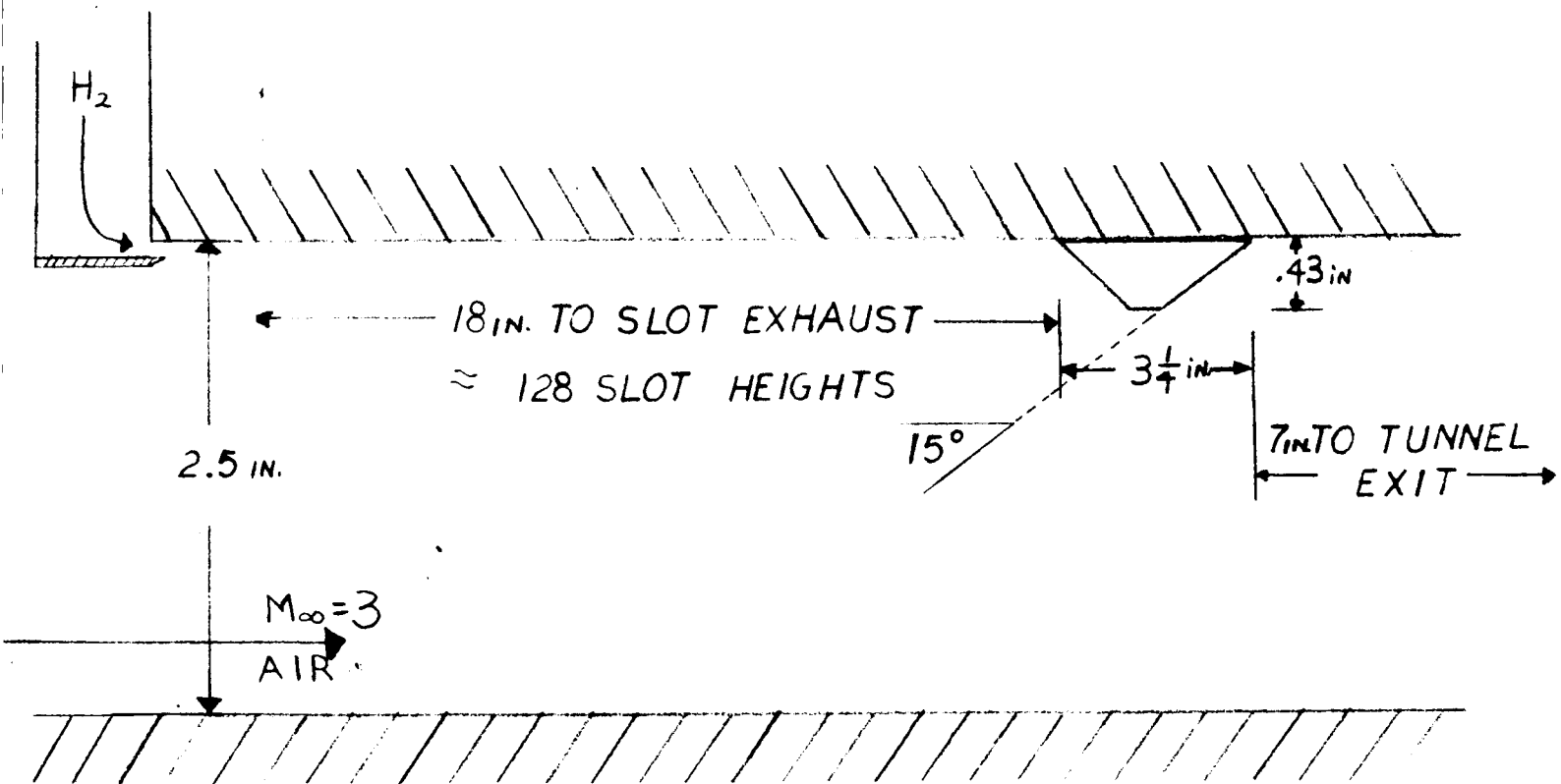


FIGURE 4

GAS HEAT TRANSFER GAUGE

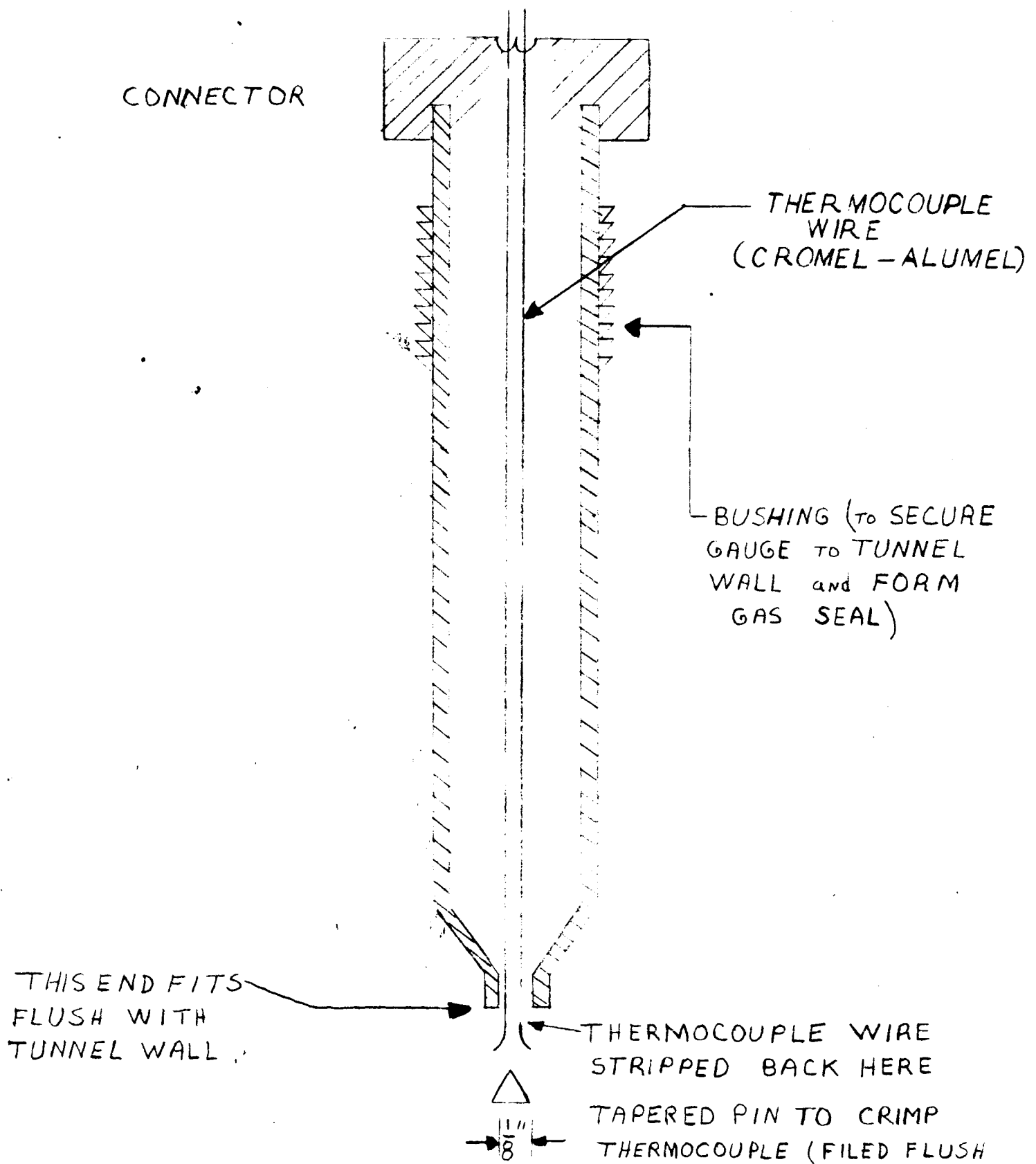
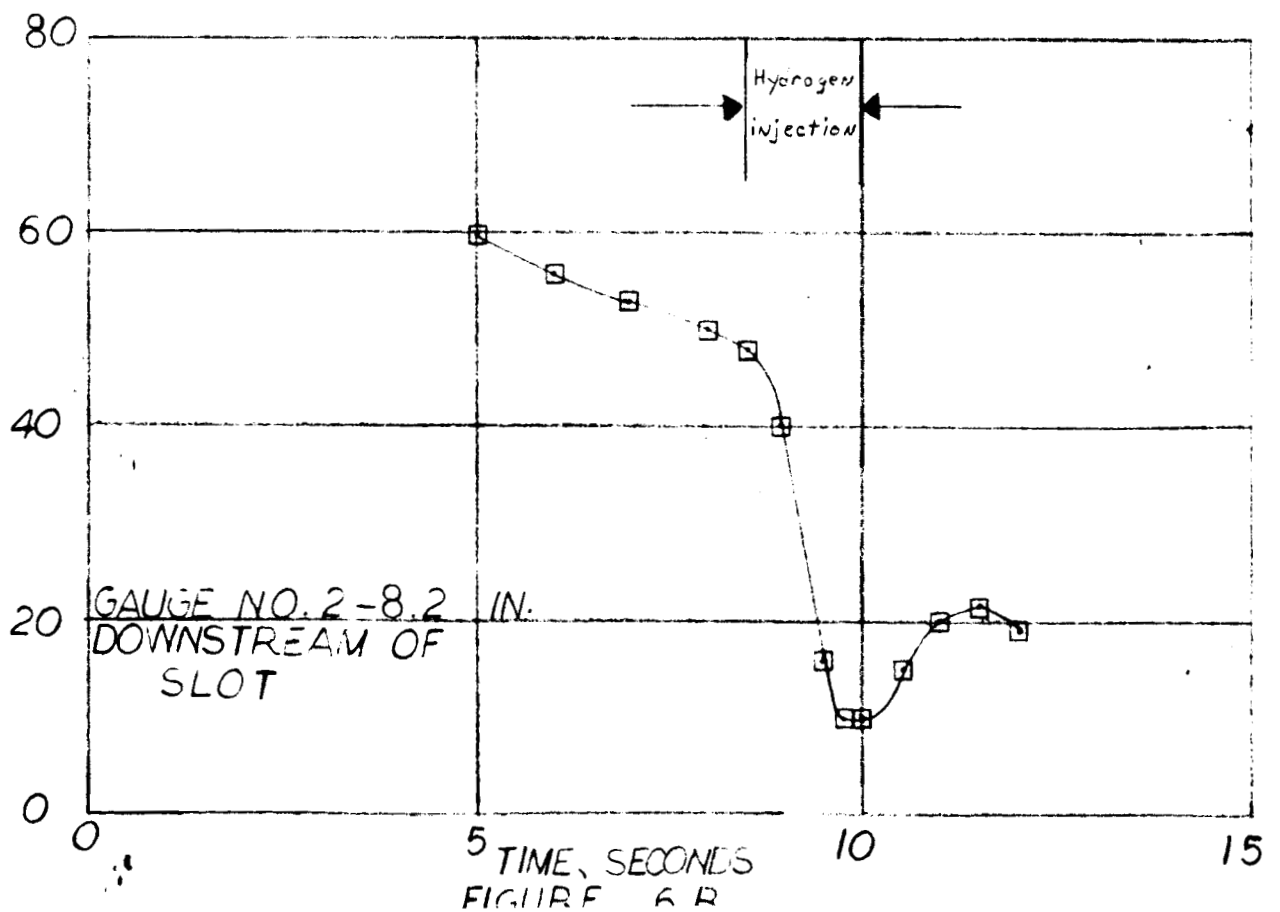
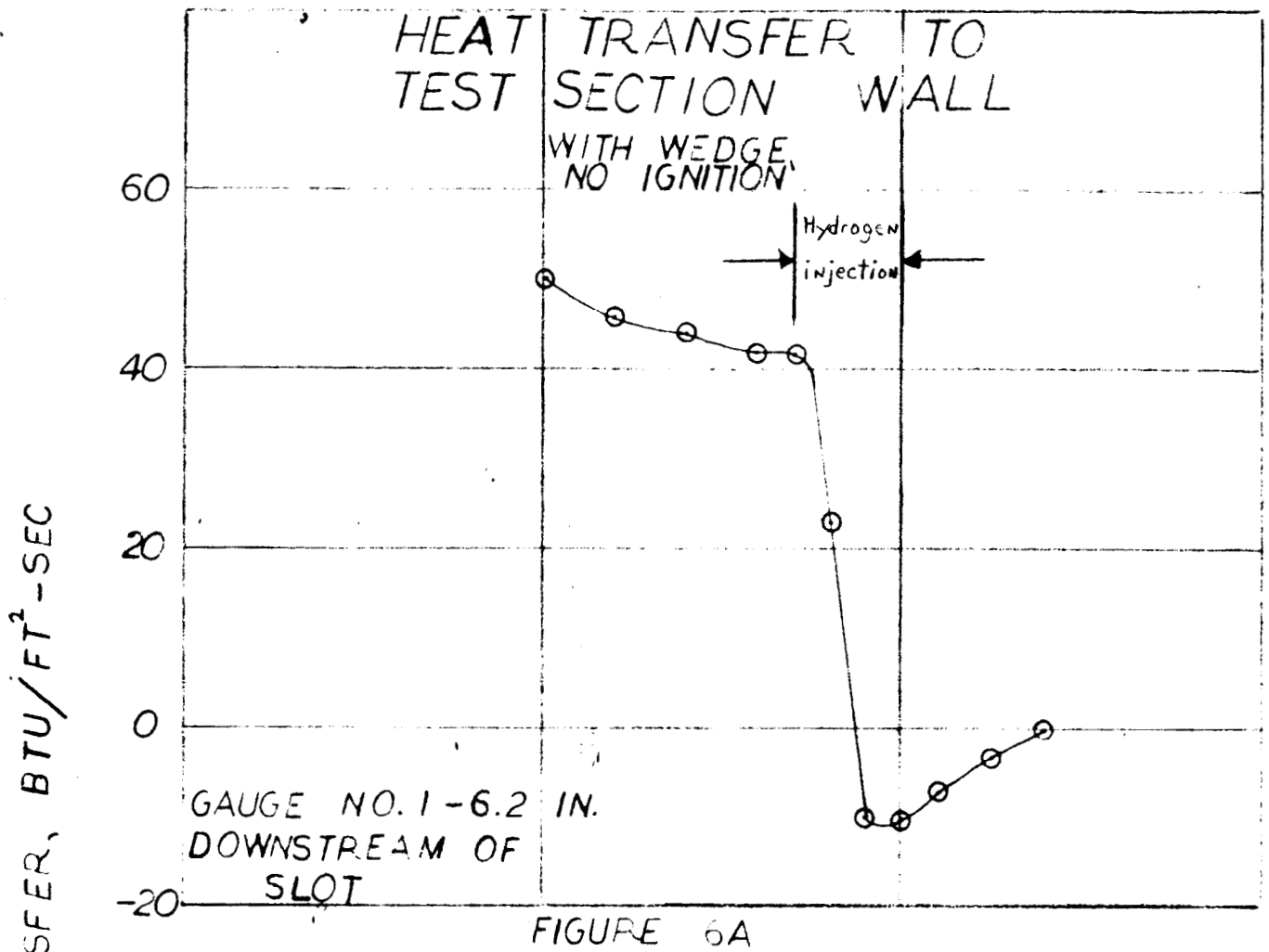
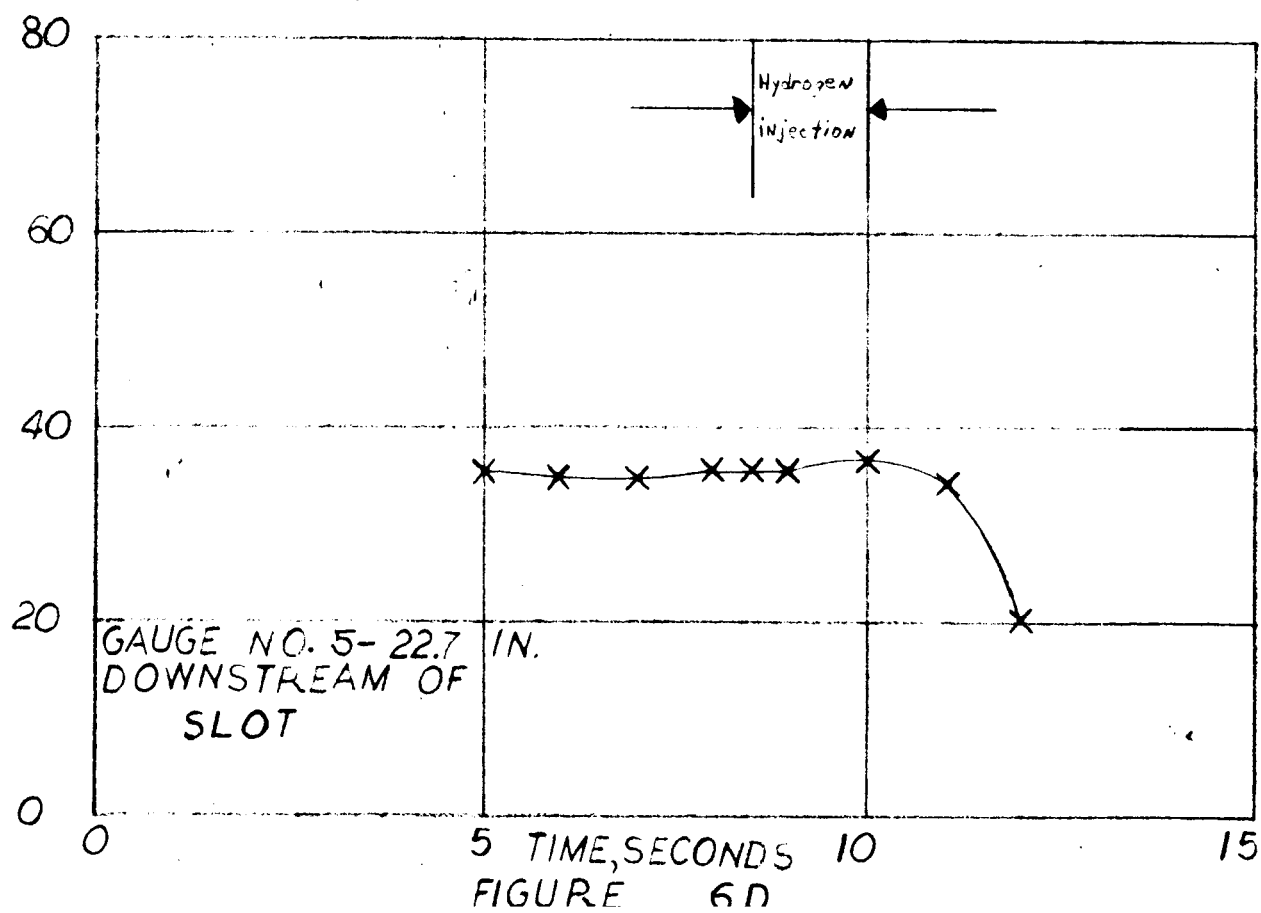
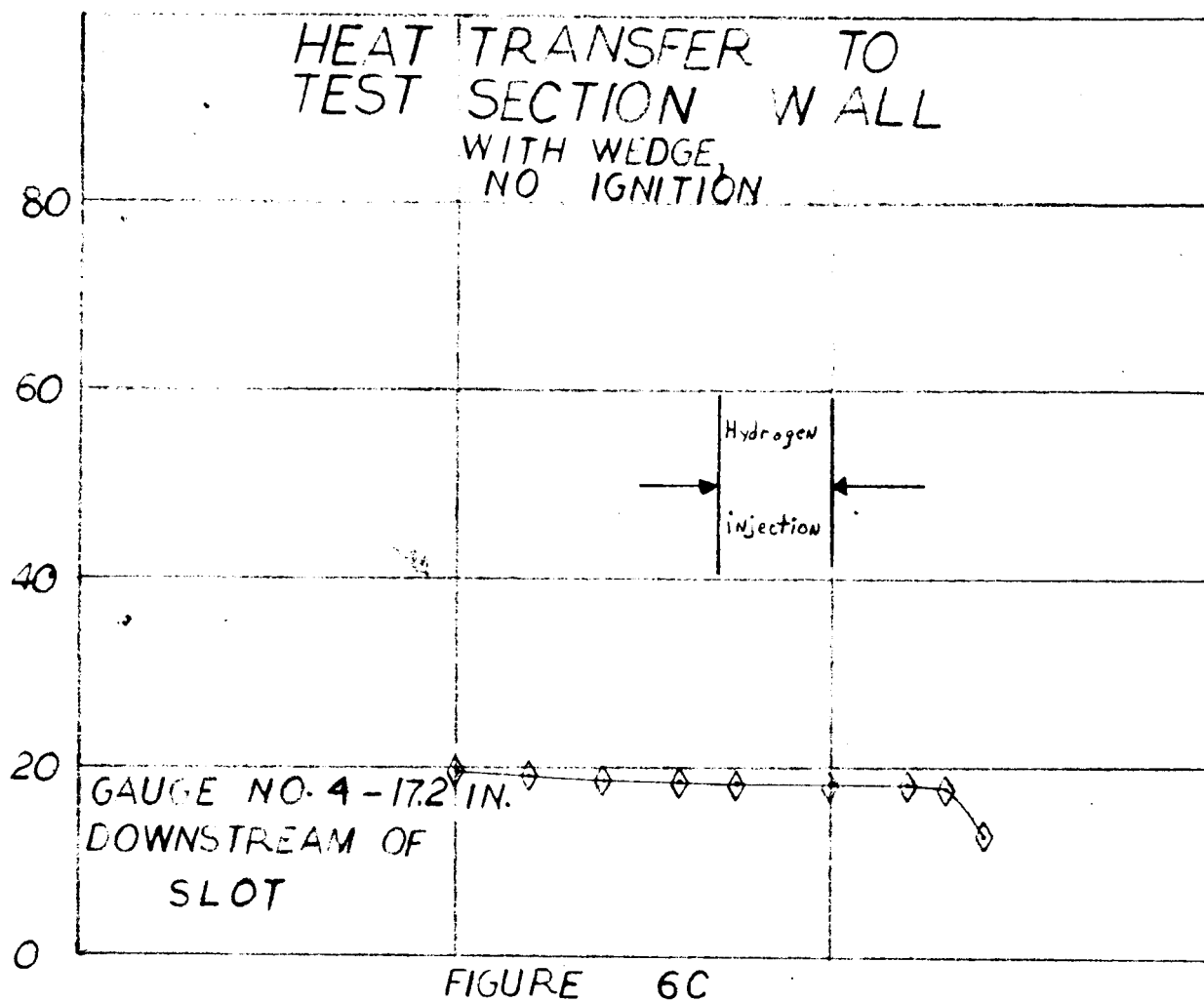
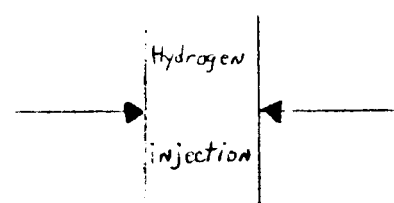


FIGURE 5



HEAT TRANSFER, BTU/FT²-SEC

HEAT TRANSFER TO TEST SECTION WALL WITH WEDGE, NO IGNITION



HEAT TRANSFER, BTU/FT²-SEC

80

60

40

20

0

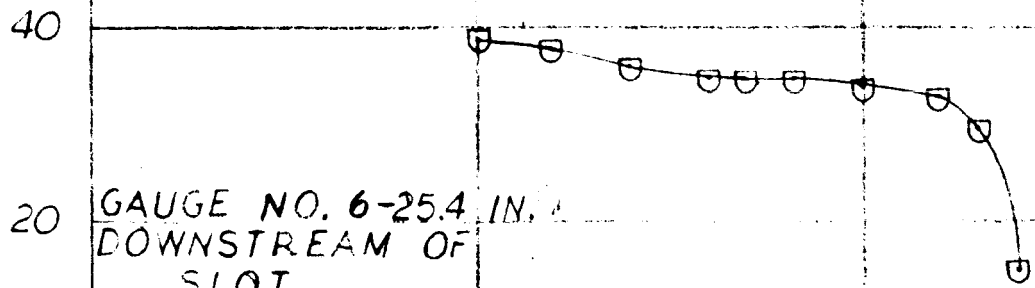
GAUGE NO. 6-25.4 IN.
DOWNSTREAM OF
SLOT

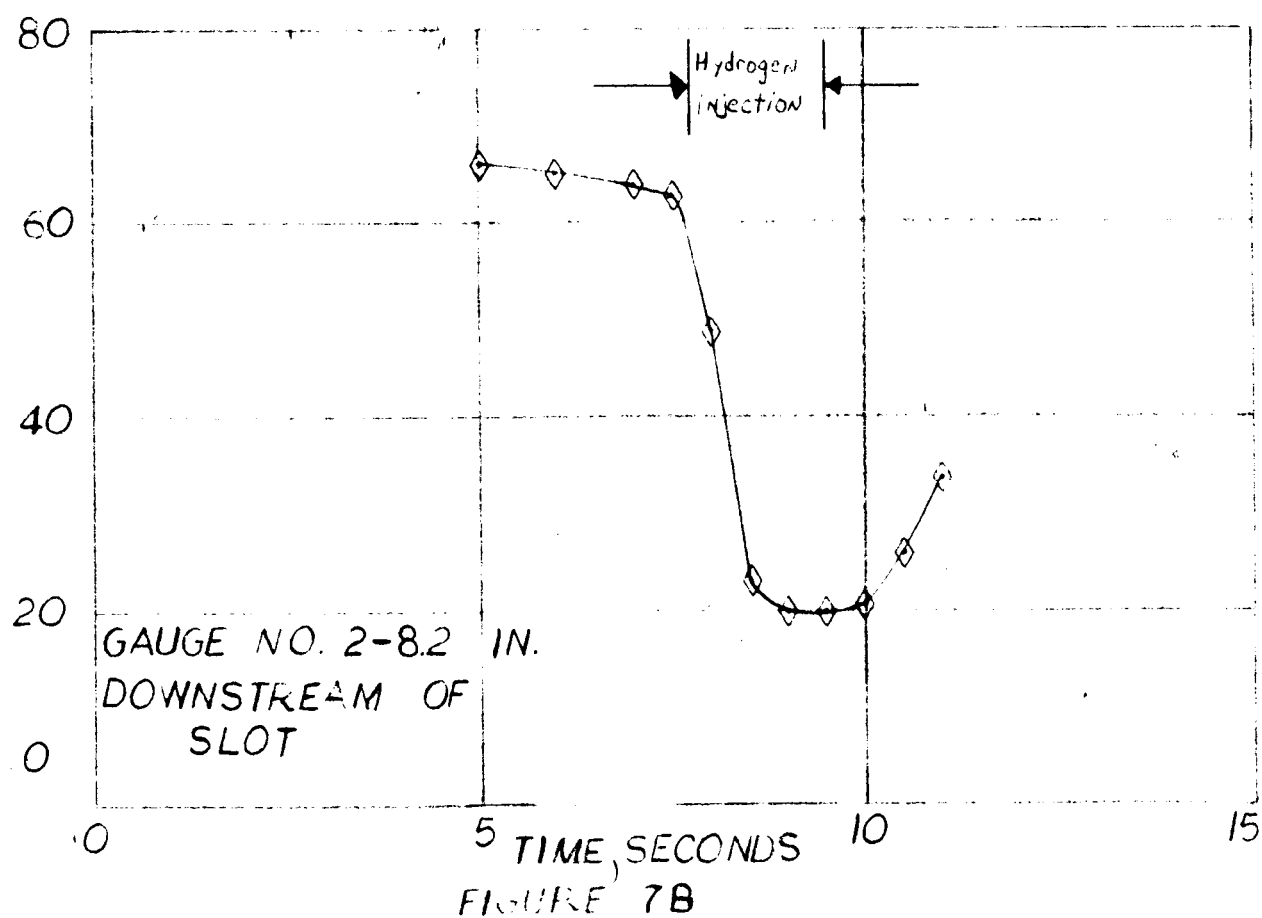
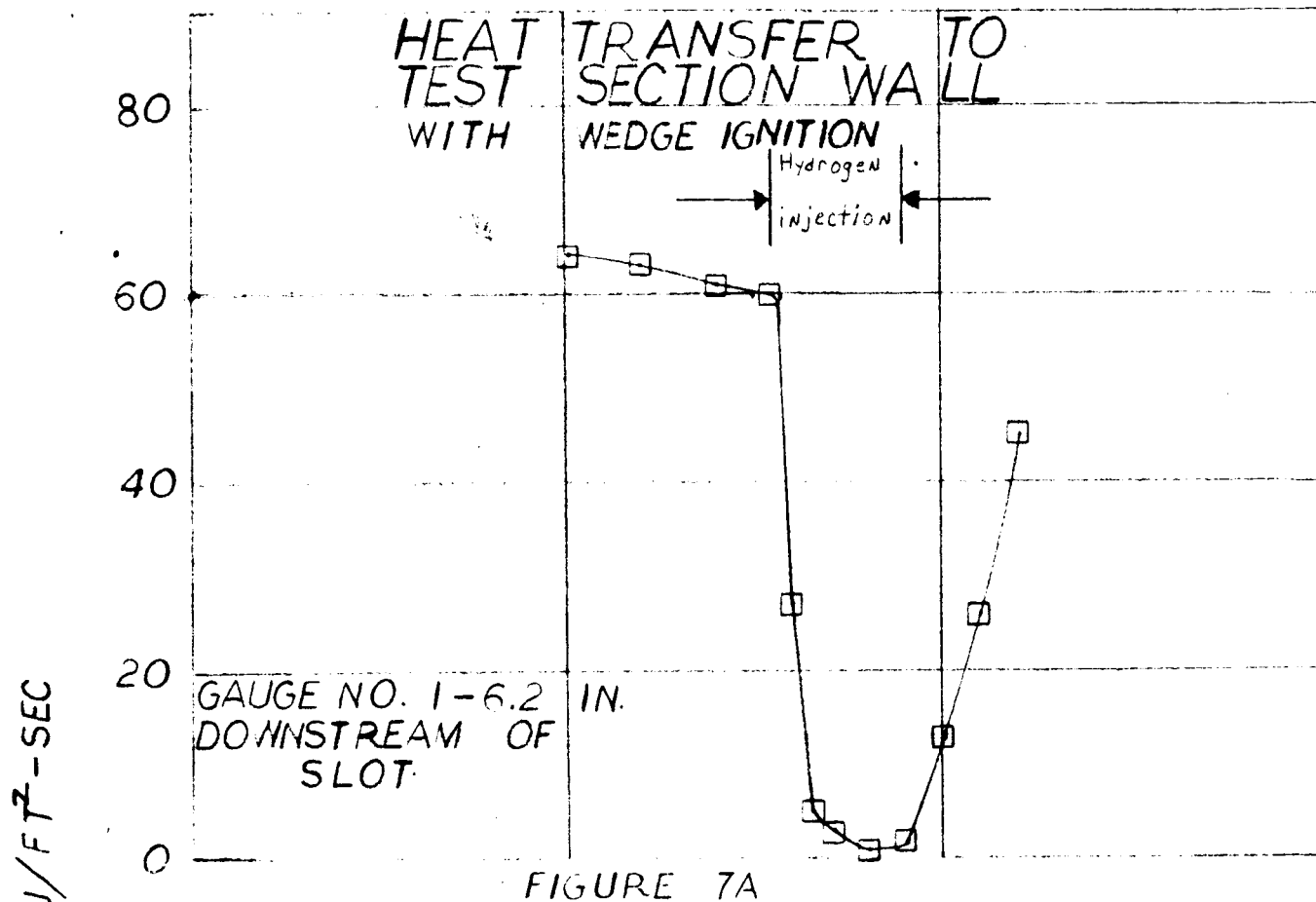
5 TIME, SECONDS

10

15

FIGURE 6E





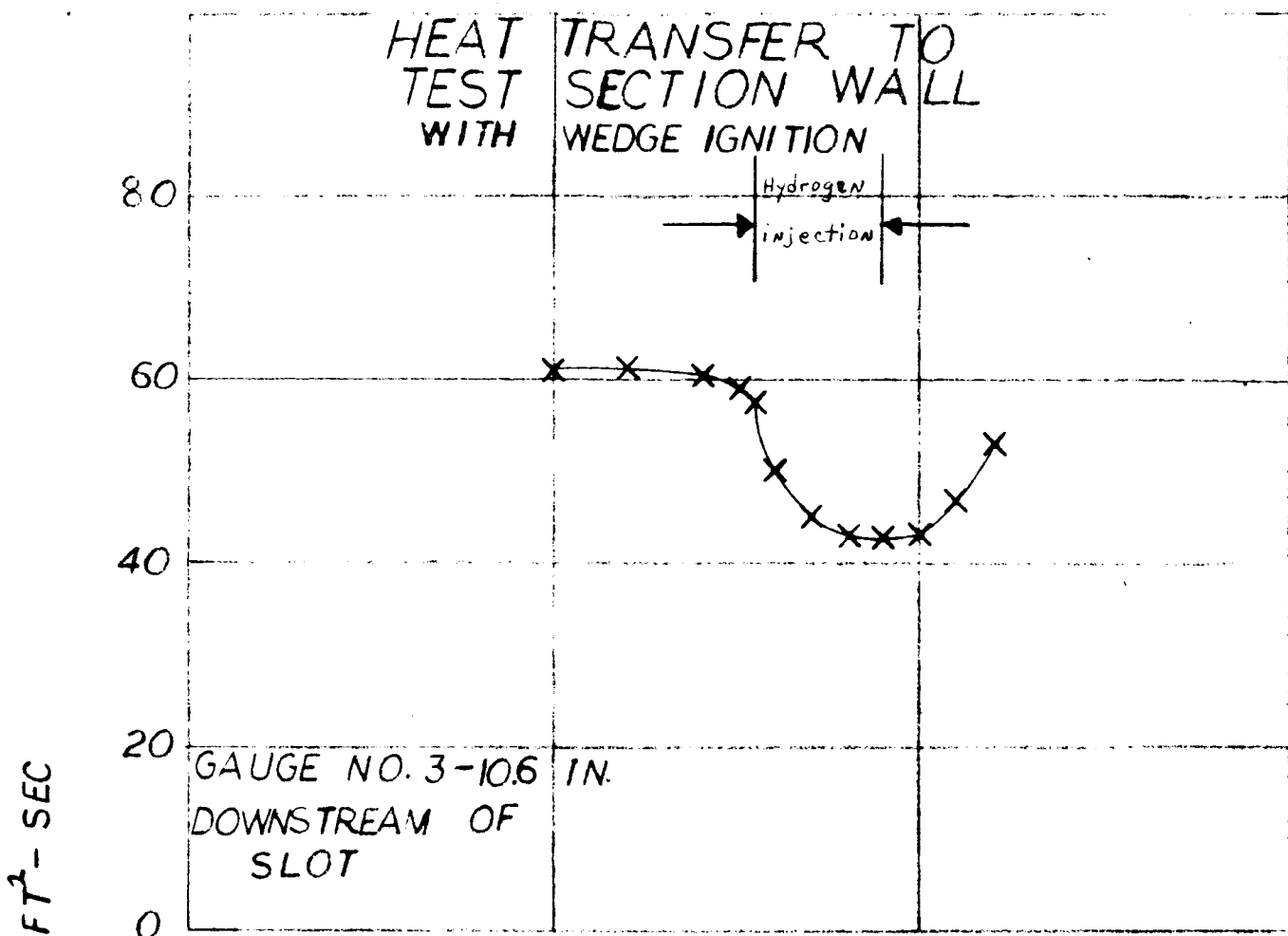


FIGURE 7C

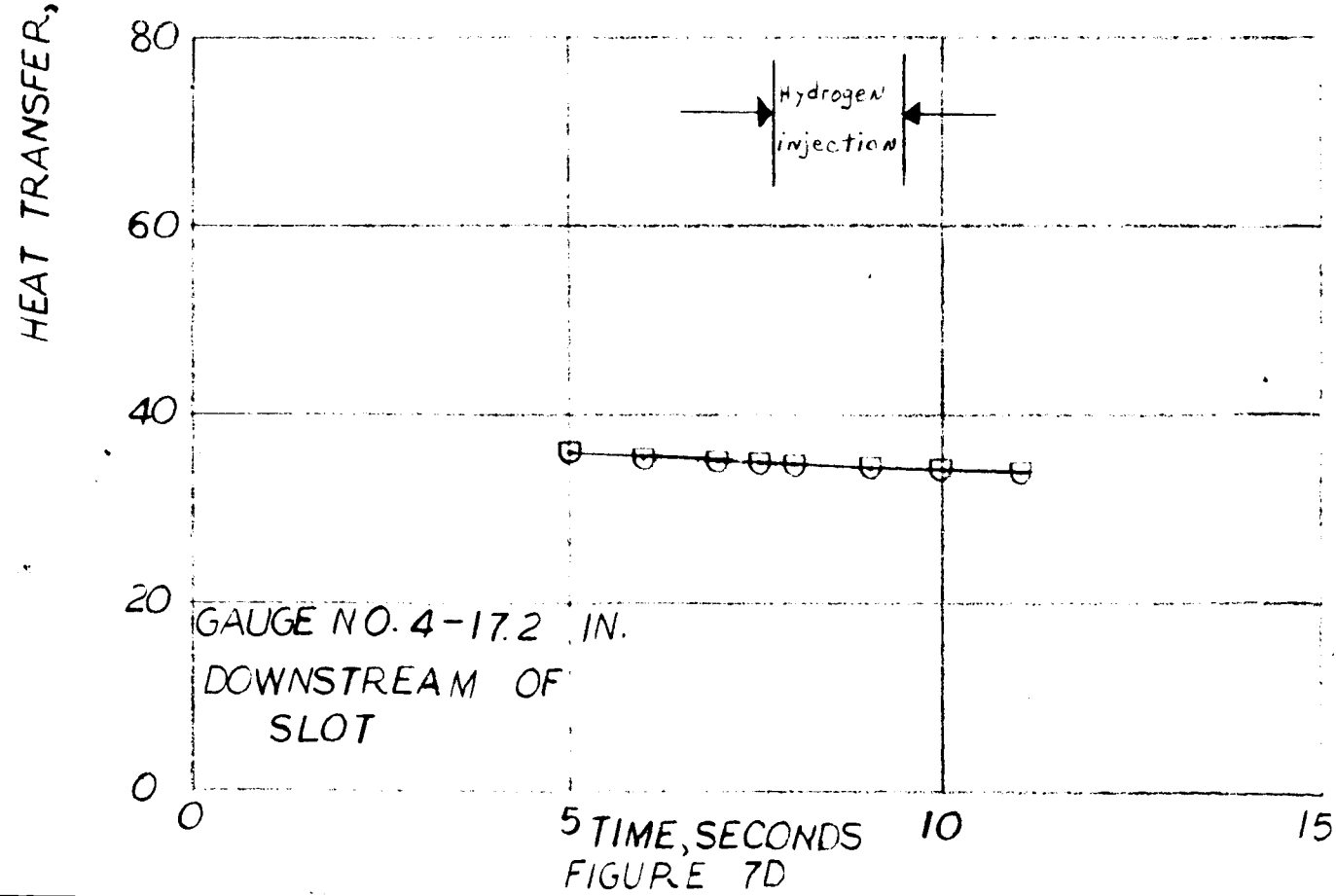


FIGURE 7D

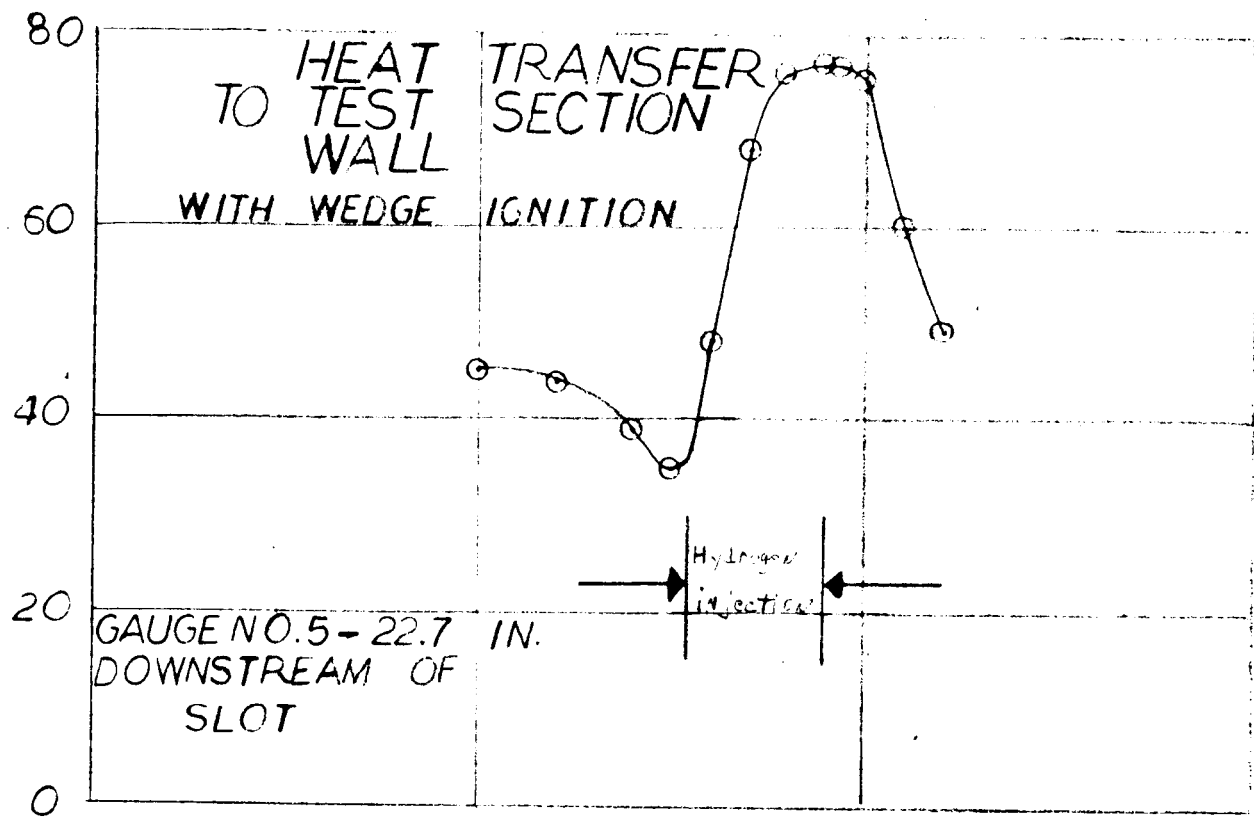


FIGURE 7E

HEAT TRANSFER, BTU/FT²-SEC

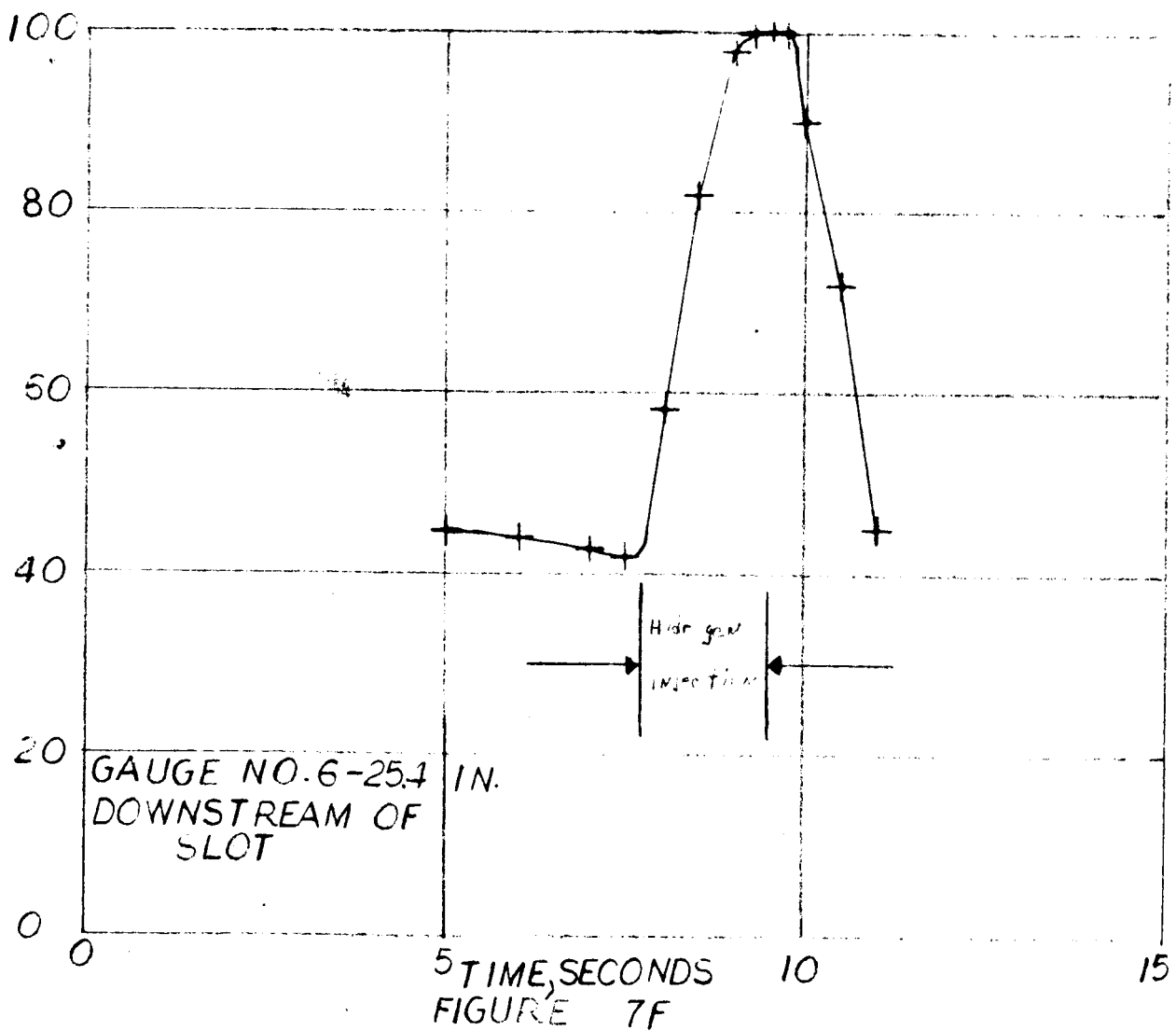
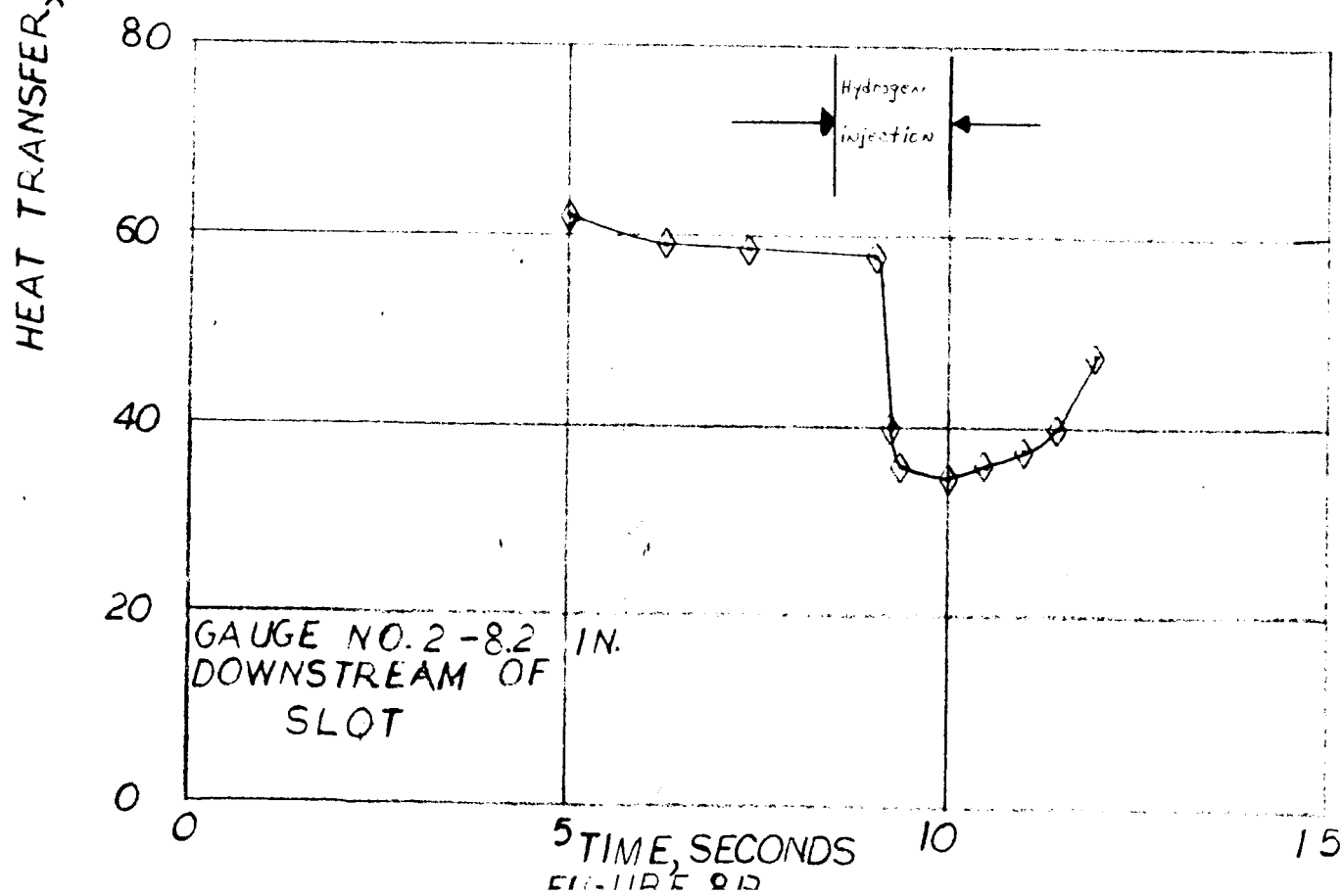
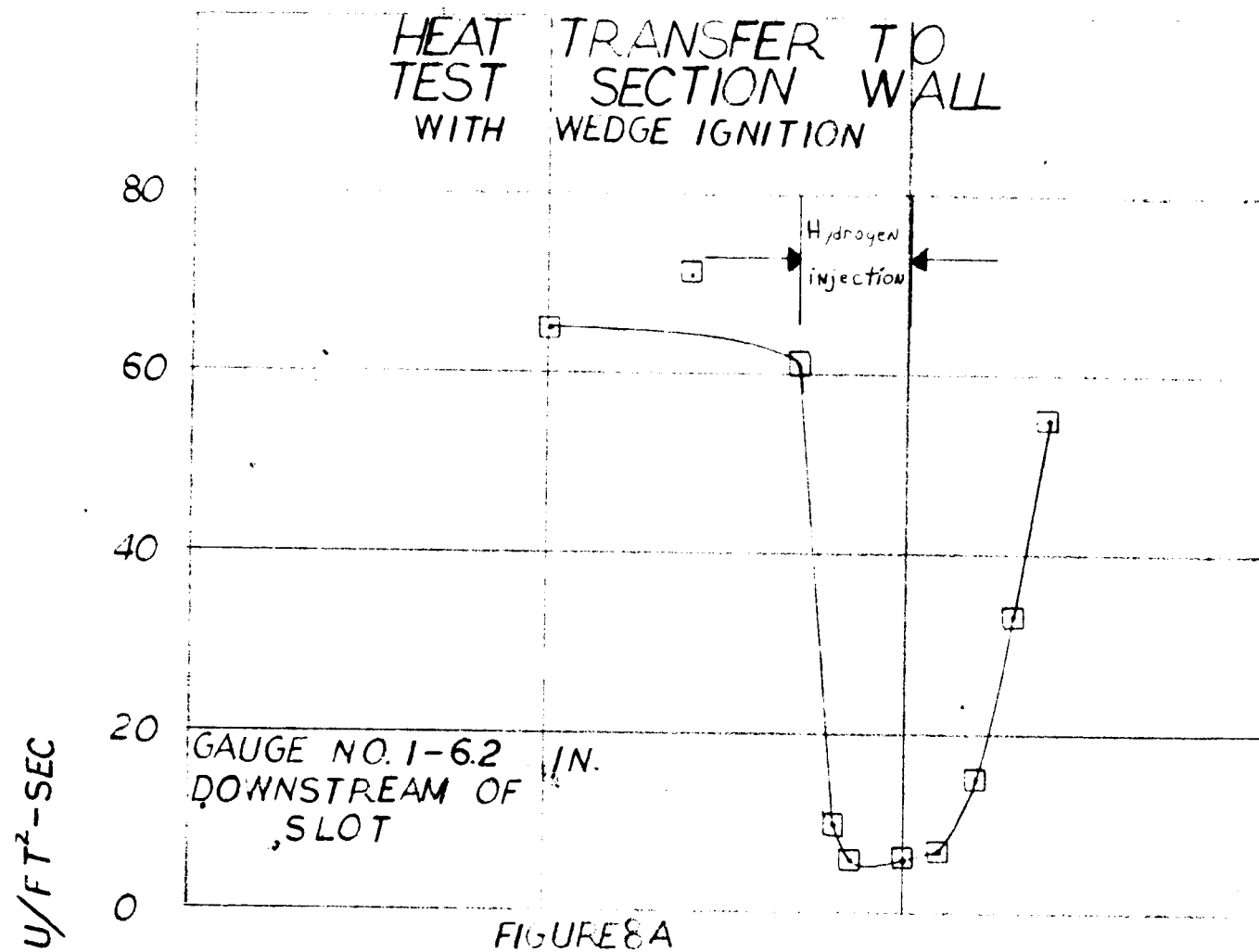


FIGURE 7F



HEAT TRANSFER TO TEST SECTION WALL WITH WEDGE IGNITION

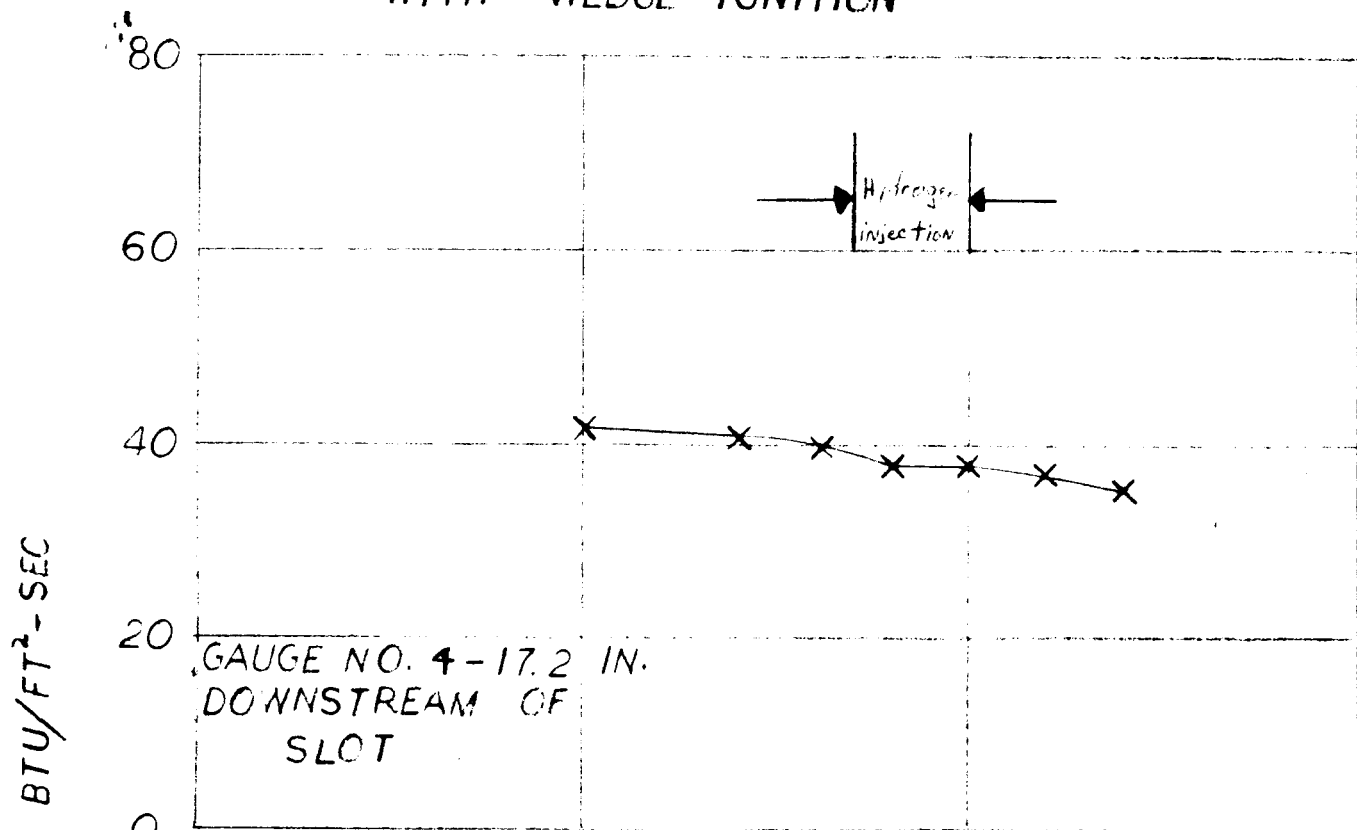


FIGURE 8C

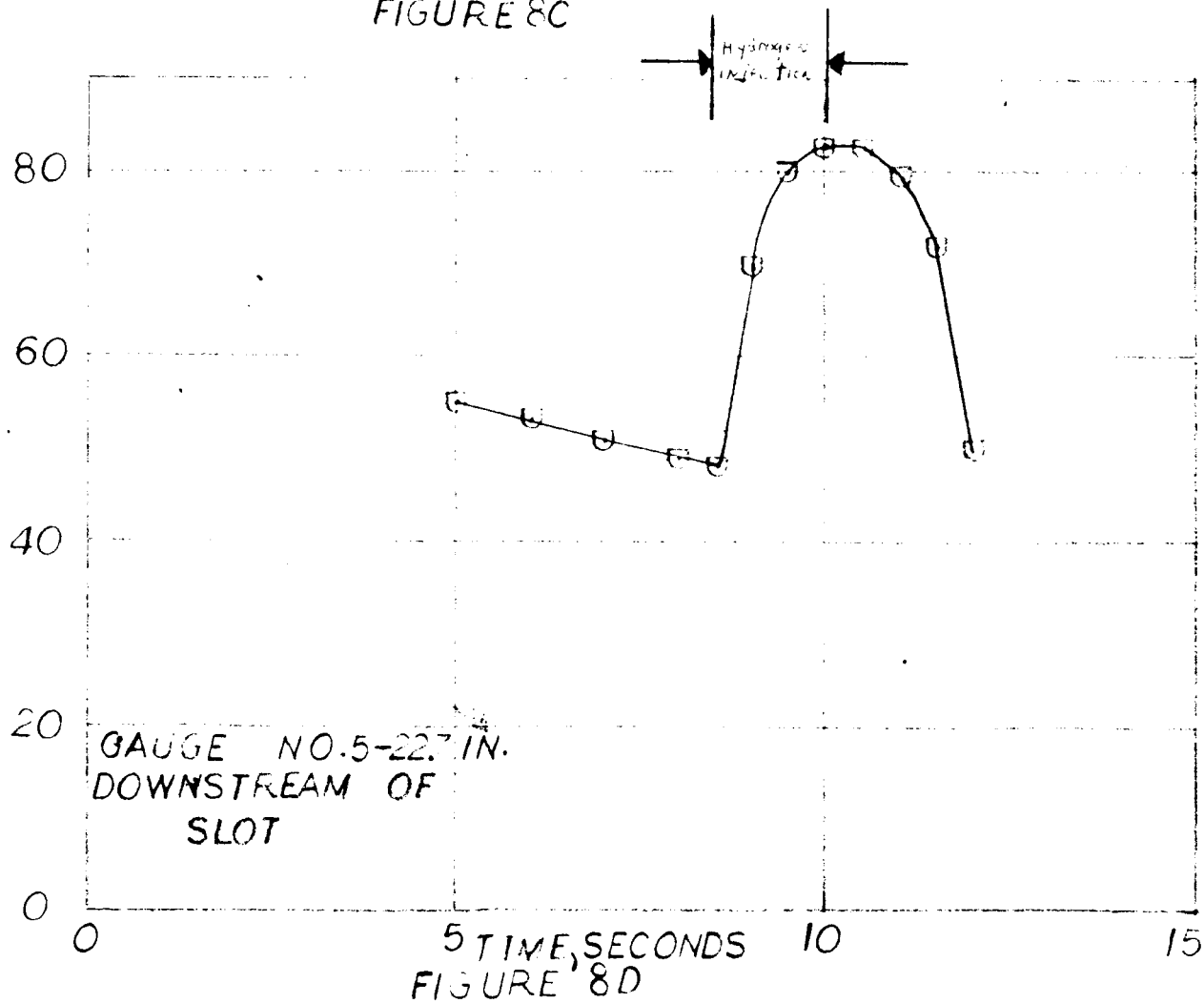
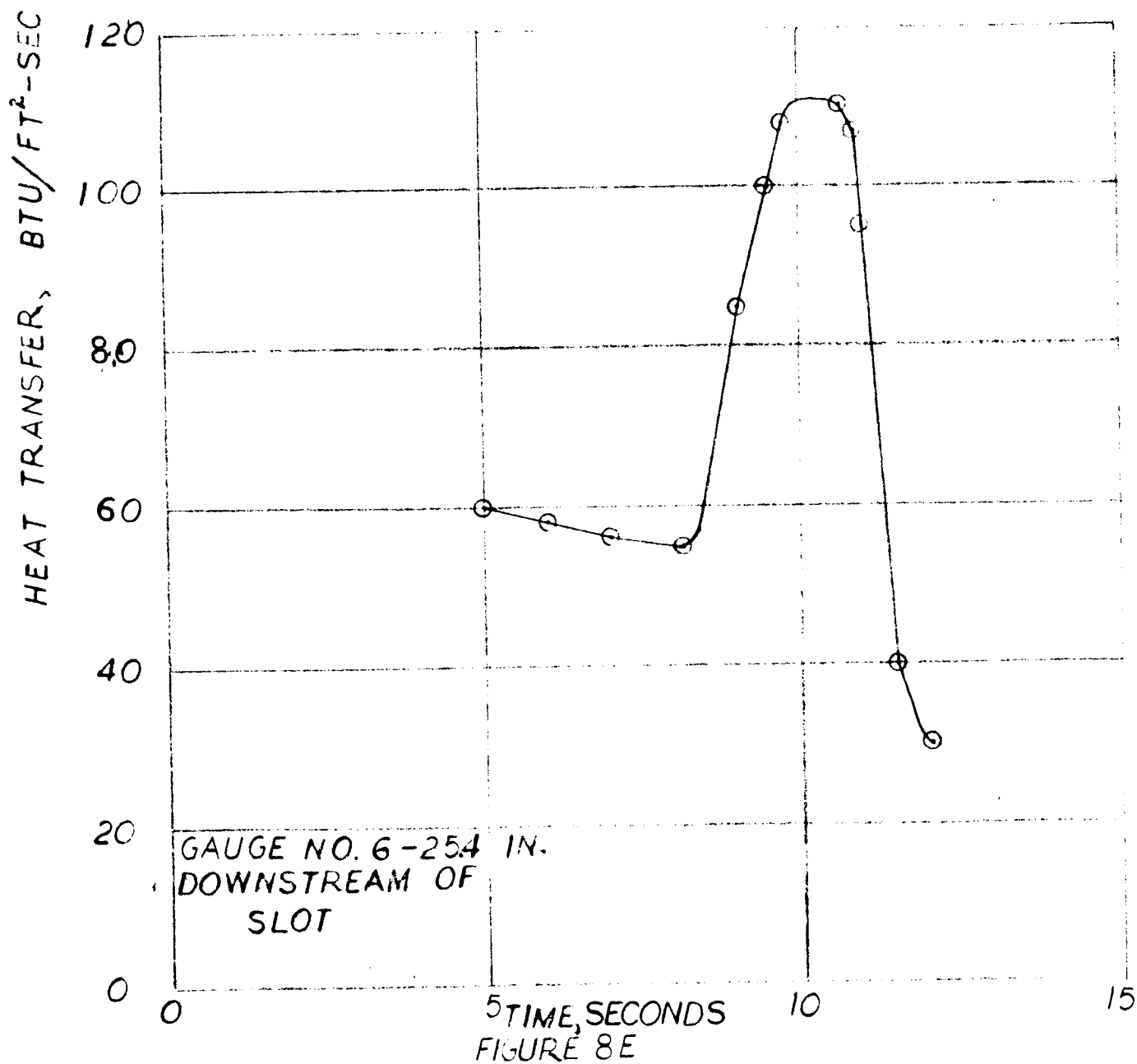
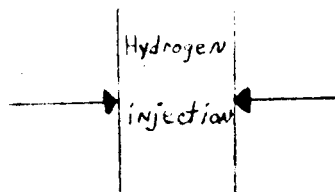


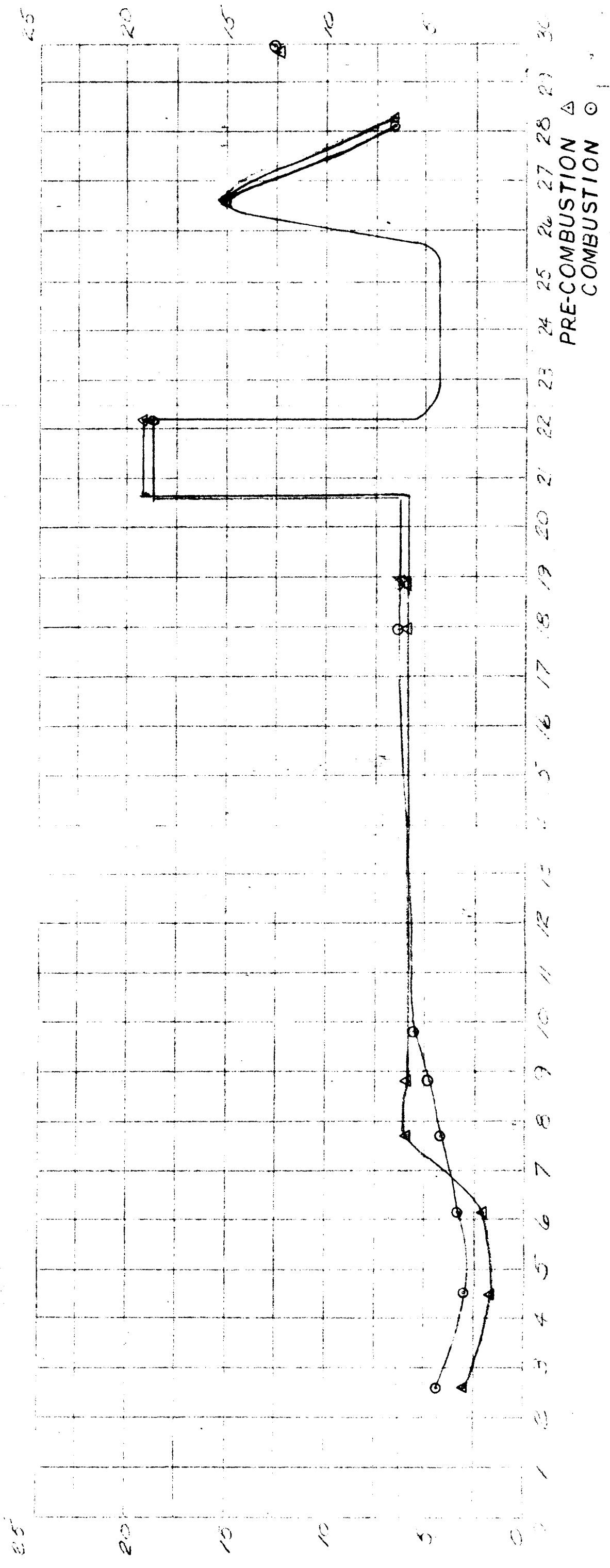
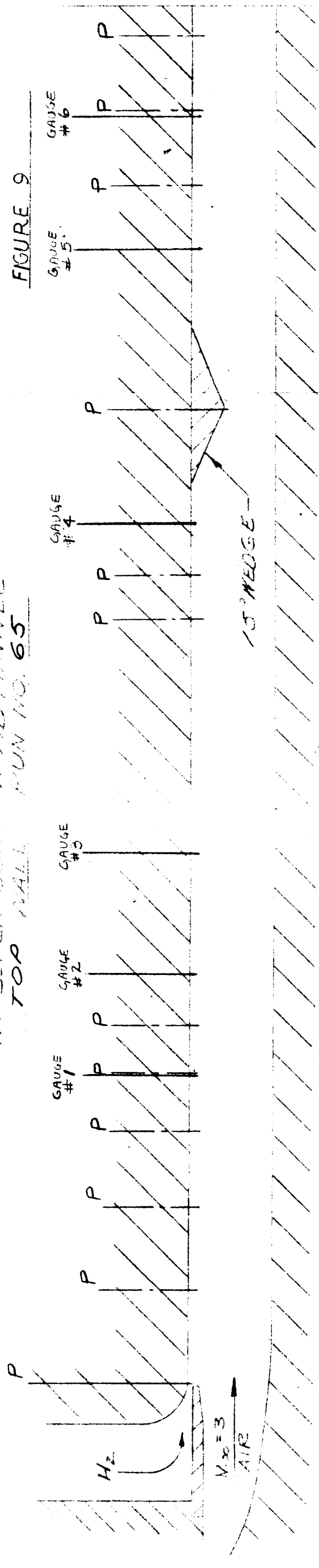
FIGURE 8D

HEAT TRANSFER TO
TEST SECTION WALL
WITH WEDGE IGNITION



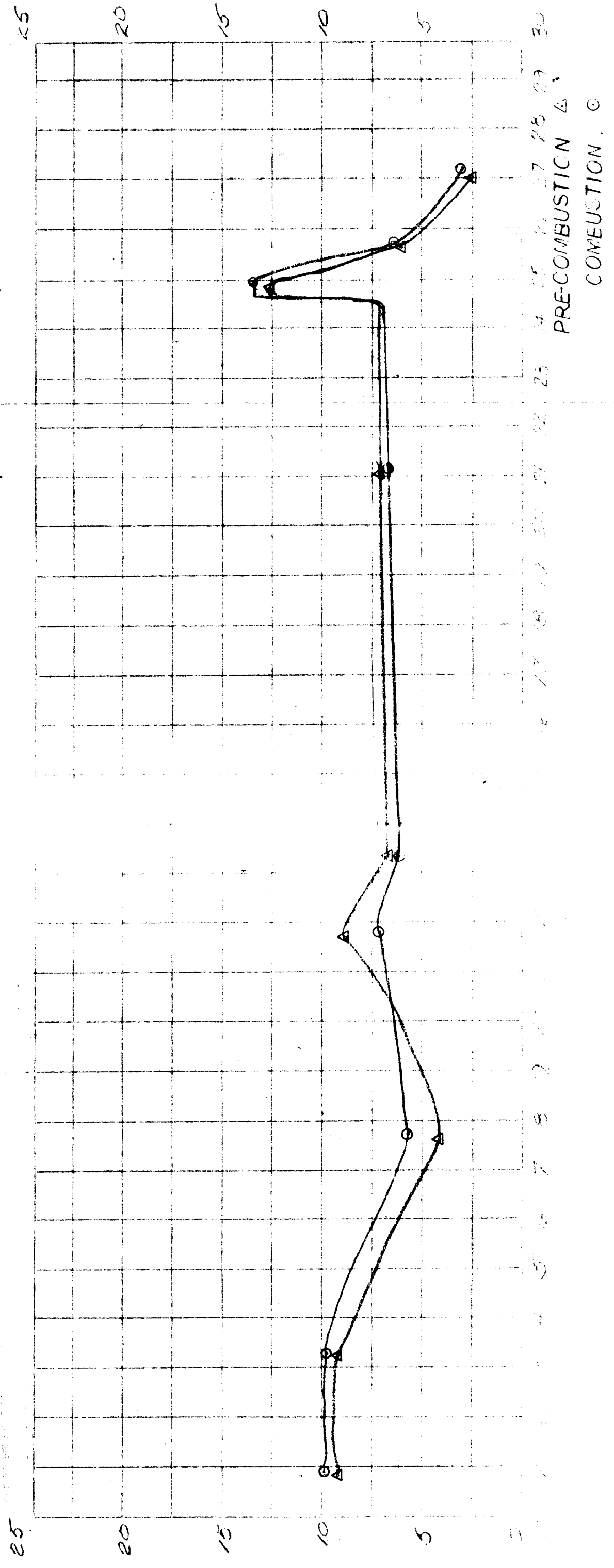
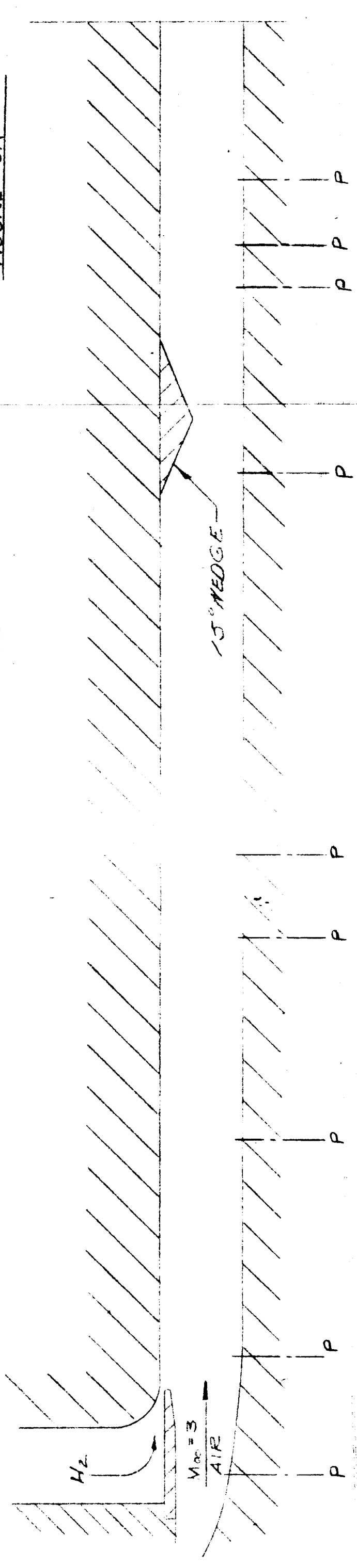
PRESSURE DISTRIBUTION
IN SUPERSONIC FLOW TUNNEL
TOP WALL RUN NO. 65

FIGURE 9

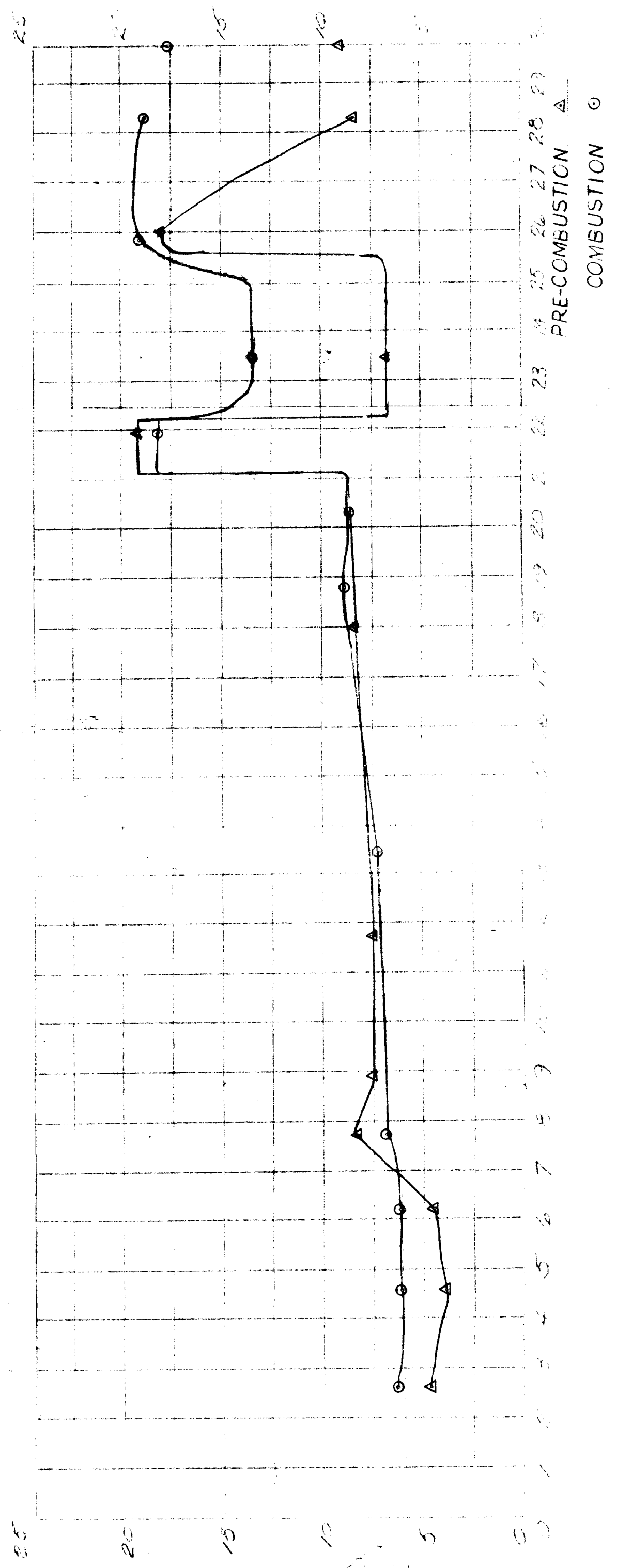
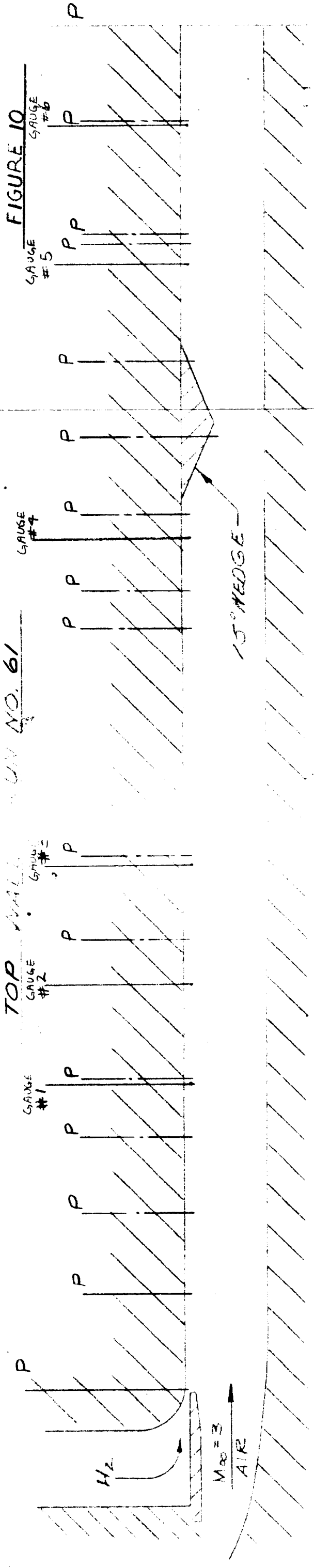


PRESSURE DISTRIBUTION
IN SUPERSONIC WIND TUNNEL
BOTTOM WALL RUN NO. 65

FIGURE 9A

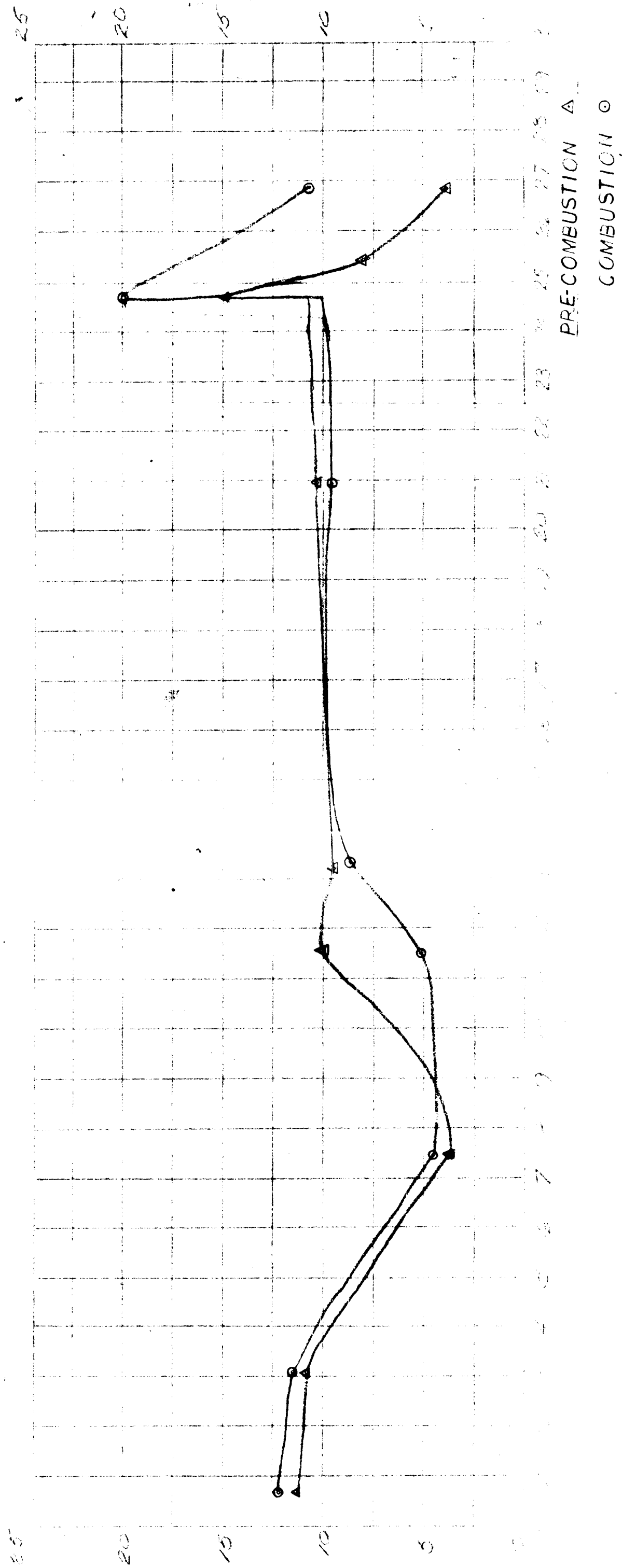
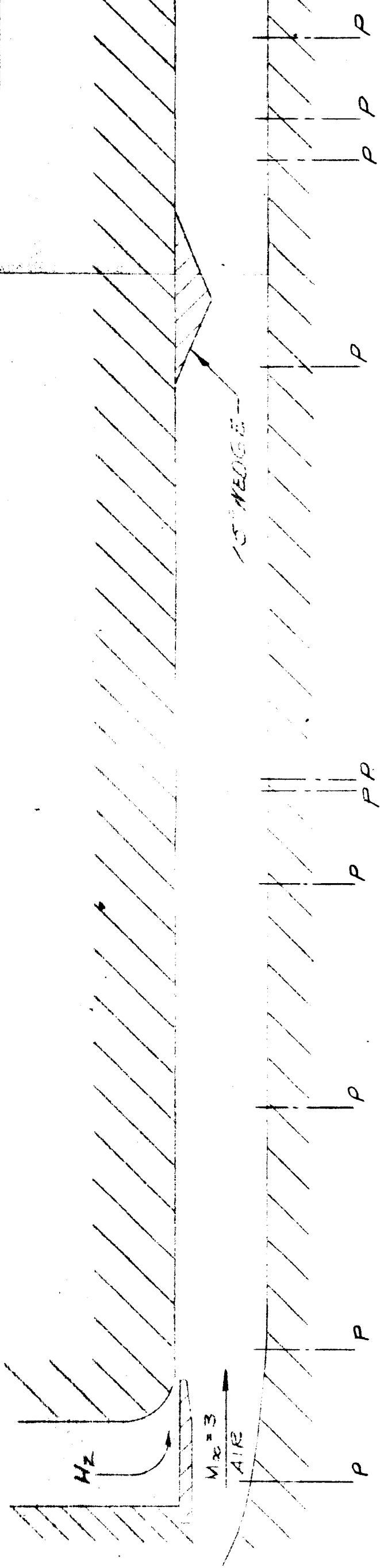


PRESSURE DISTRIBUTION
IN SUPERSONIC WIND TUNNEL
TUN NO. 61



PRESSURE DISTRIBUTION
IN SUPER SONIC WIND TUNNEL
BOTTOMWALL RUN NO. 61

FIGURE 10A



PRE-COMBUSTION A

COMBUSTION ©

PRESSURE DISTRIBUTION
IN SUPERSONIC WIND TUNNEL
TOP WALL RUN NO. 62

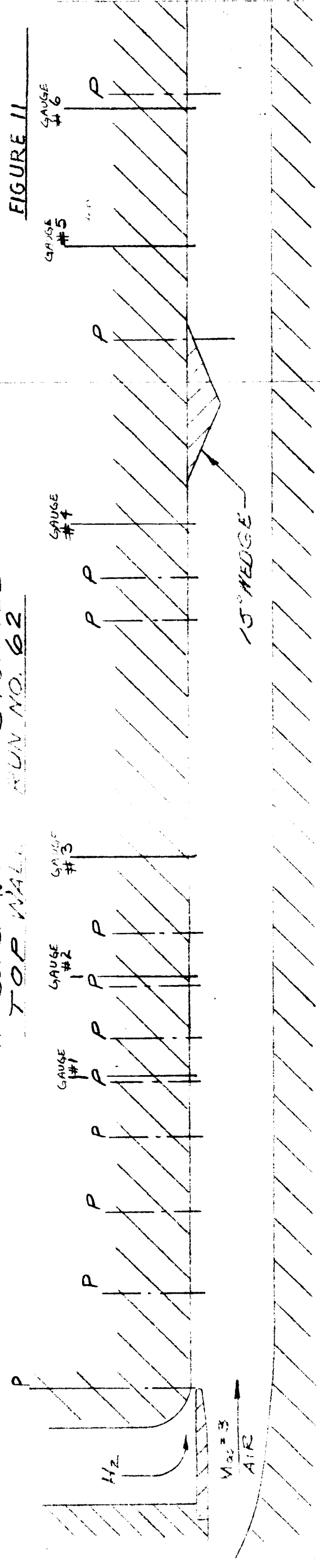
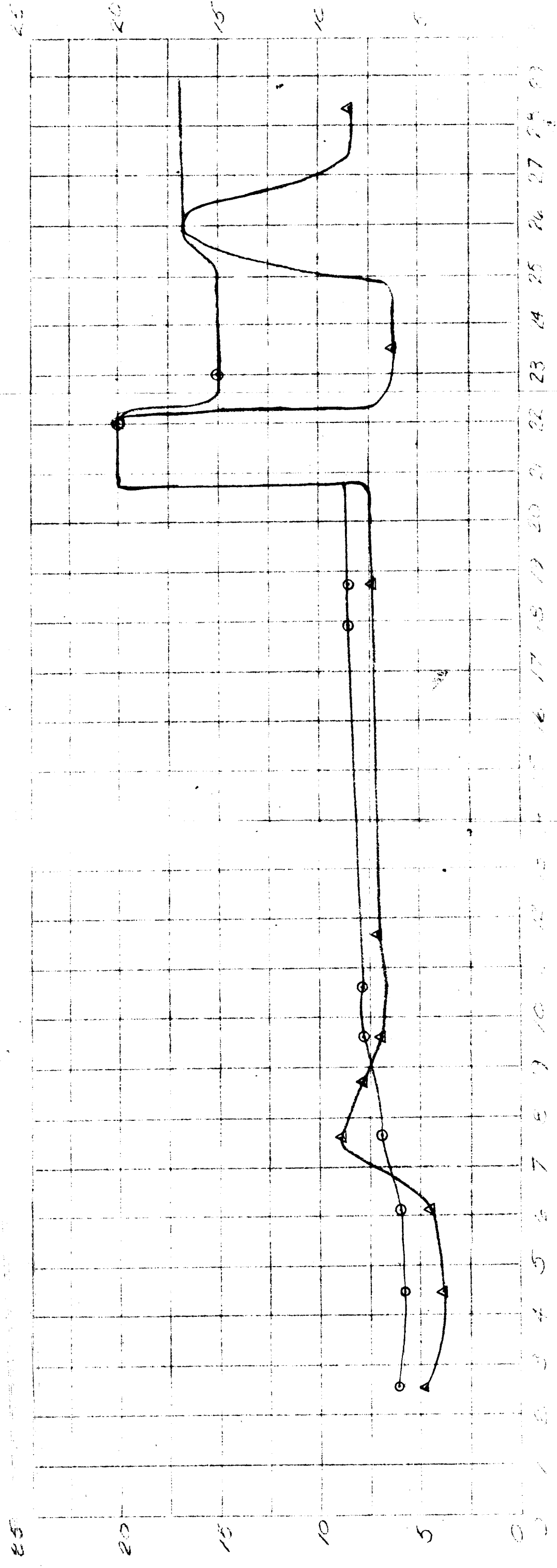


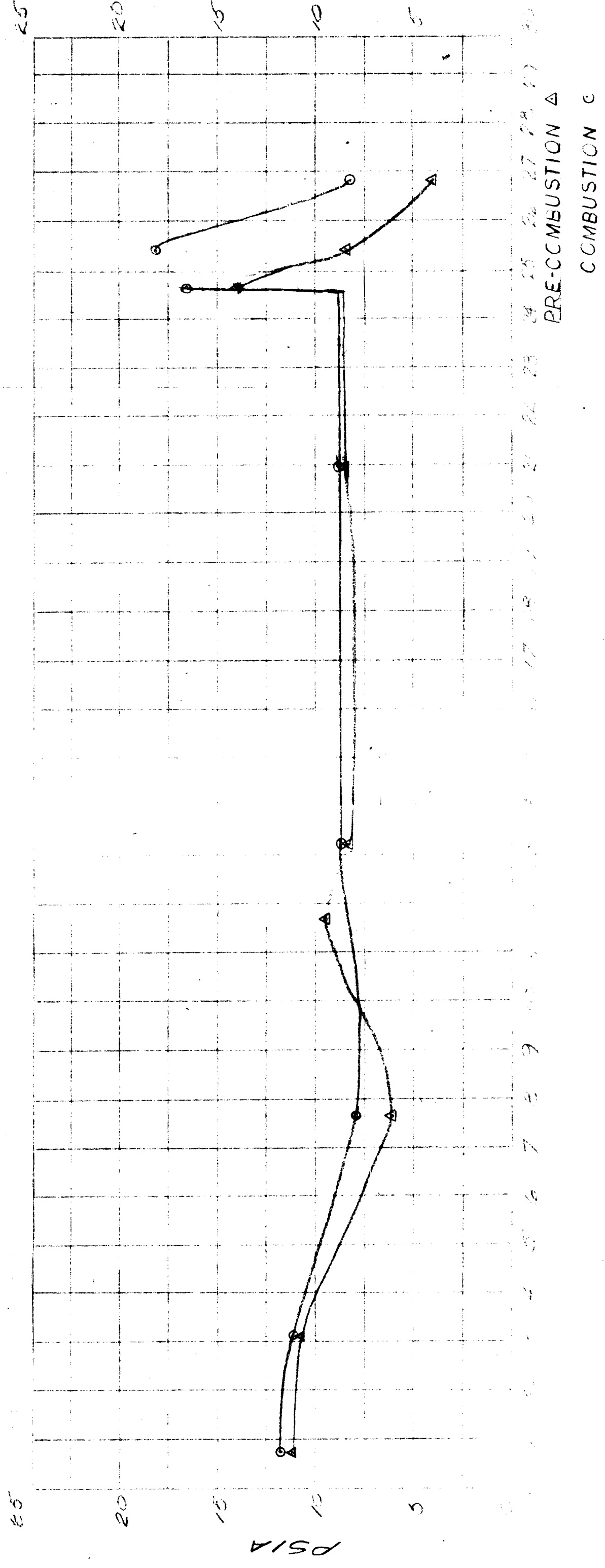
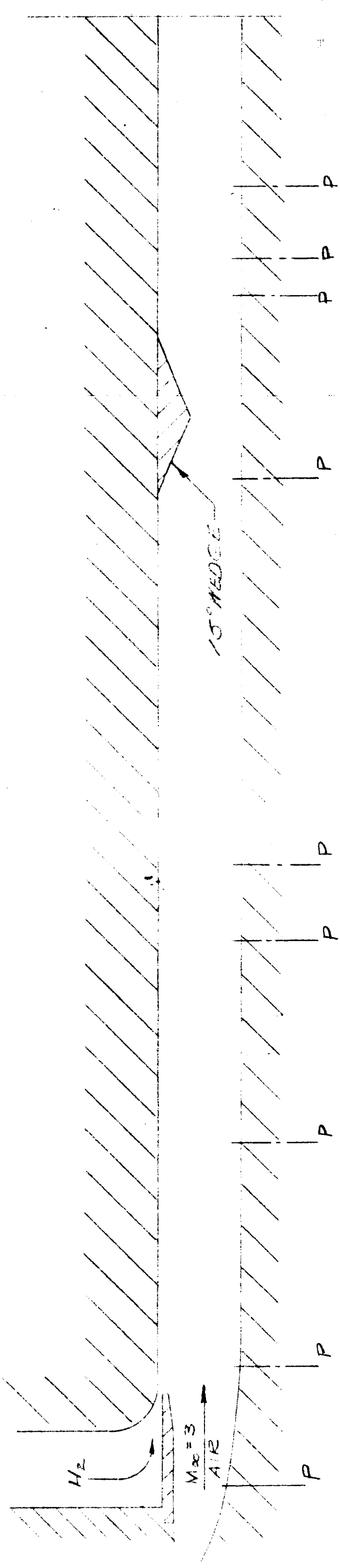
FIGURE 11



PRE-COMBUSTION
COMBUSTION

PRESSURE DISTRIBUTION
IN SUPERSONIC WIND TUNNEL
BOTTOM WALL RUN NO. 62

FIGURE IIA



LUMINOSITY PHOTOGRAPH OF
IGNITION ON WEDGE

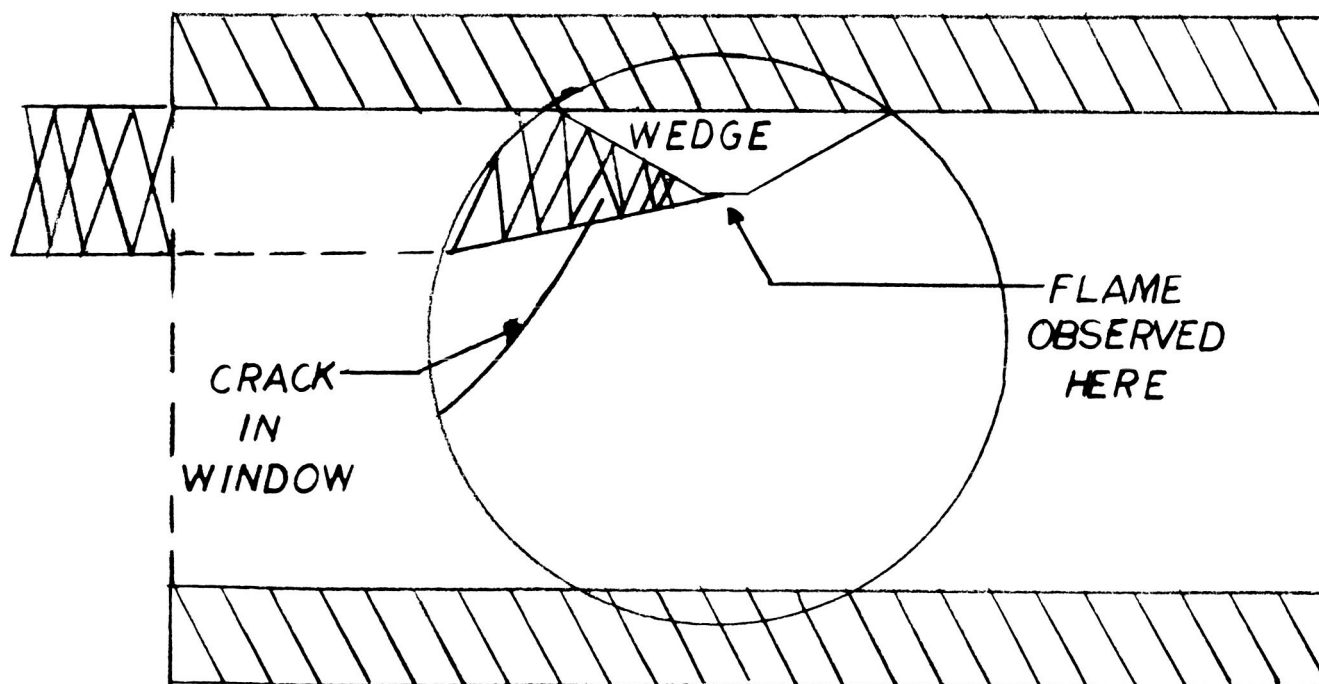
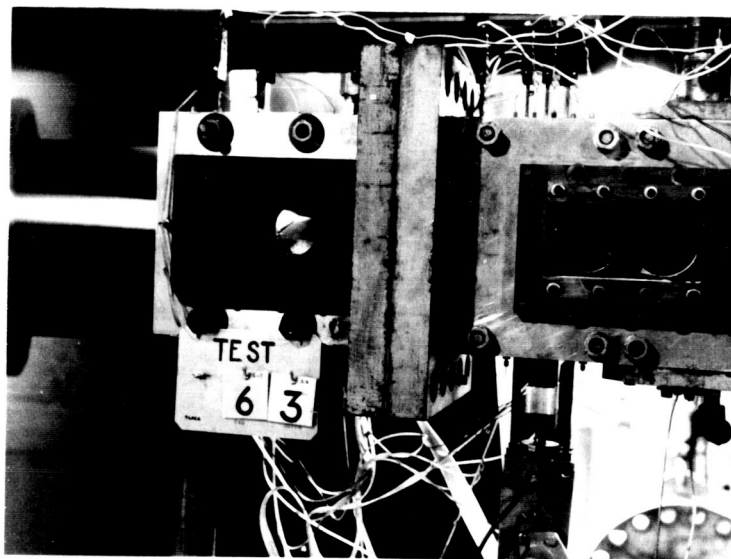


FIGURE 12

LUMINOSITY PHOTOGRAPH OF
BURNING TRIGGERED BY
DISTURBANCE

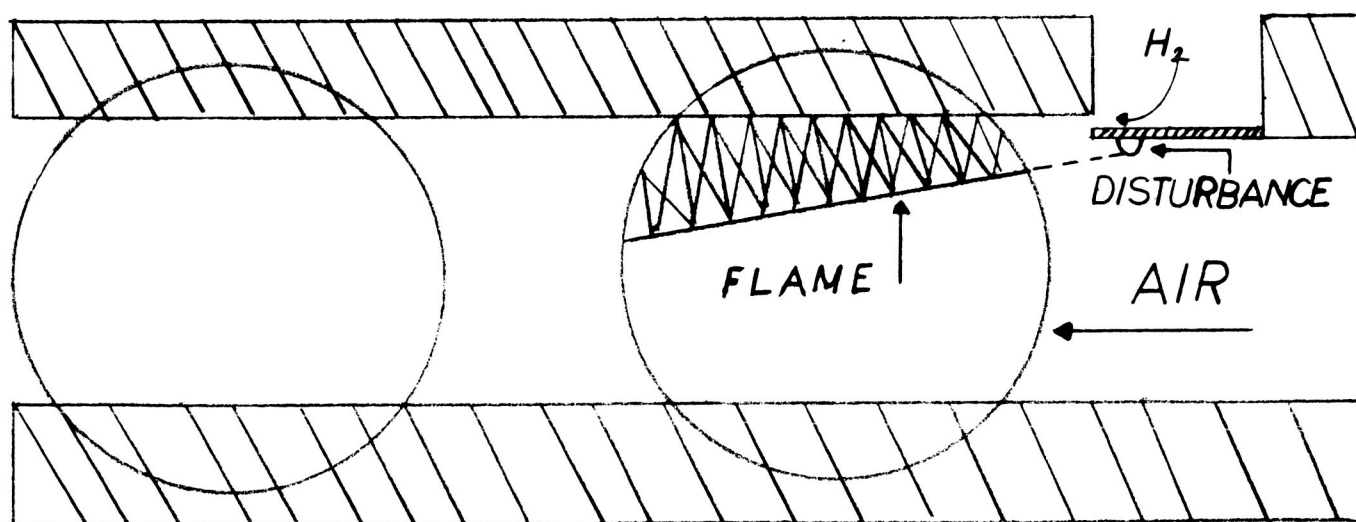
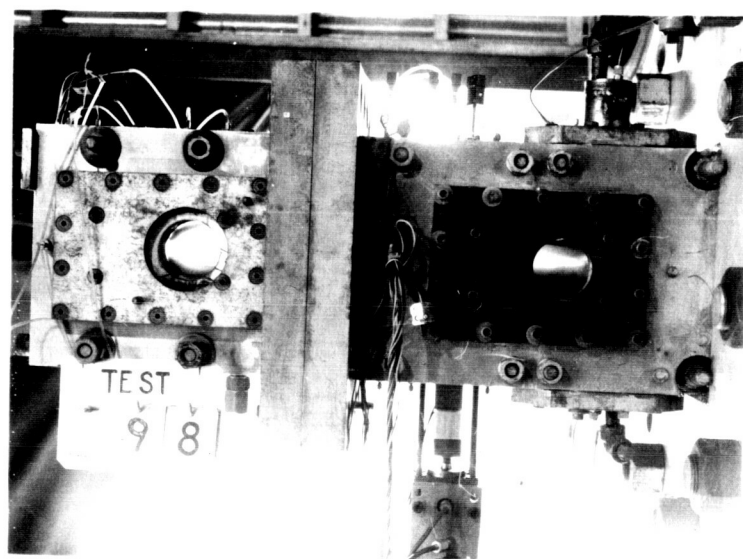
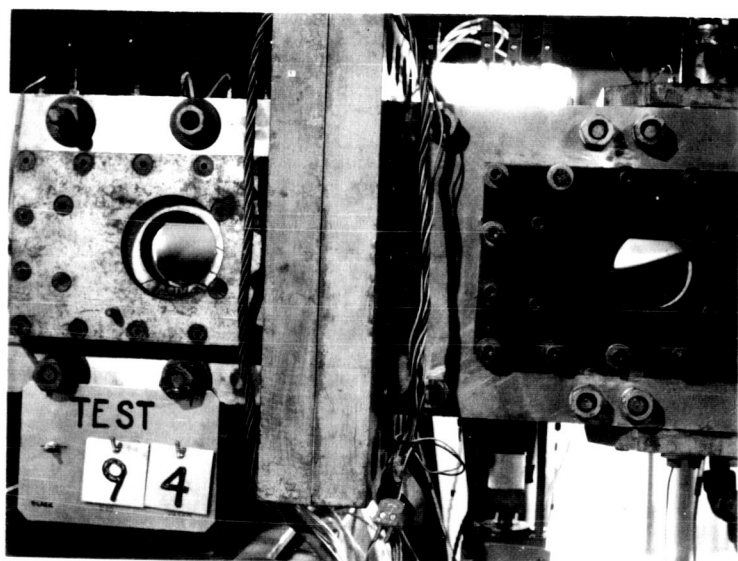
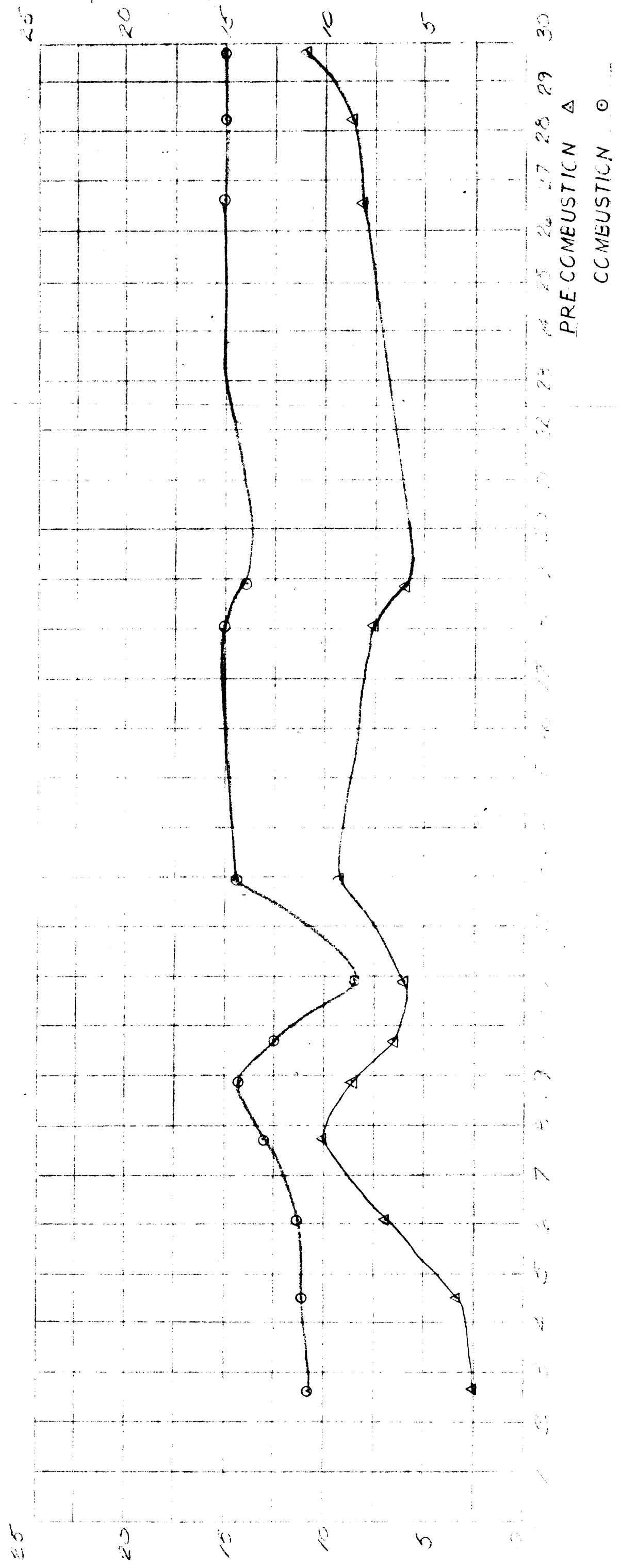
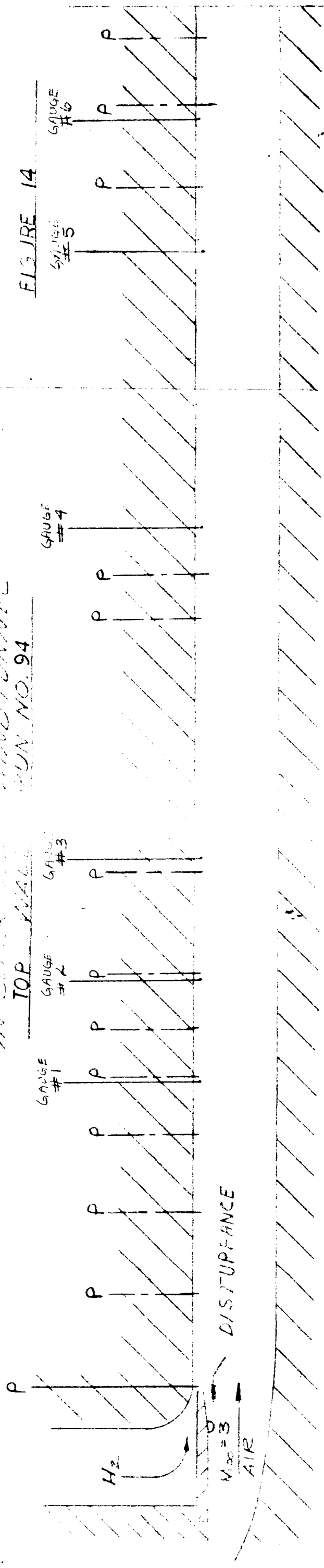


FIGURE 13

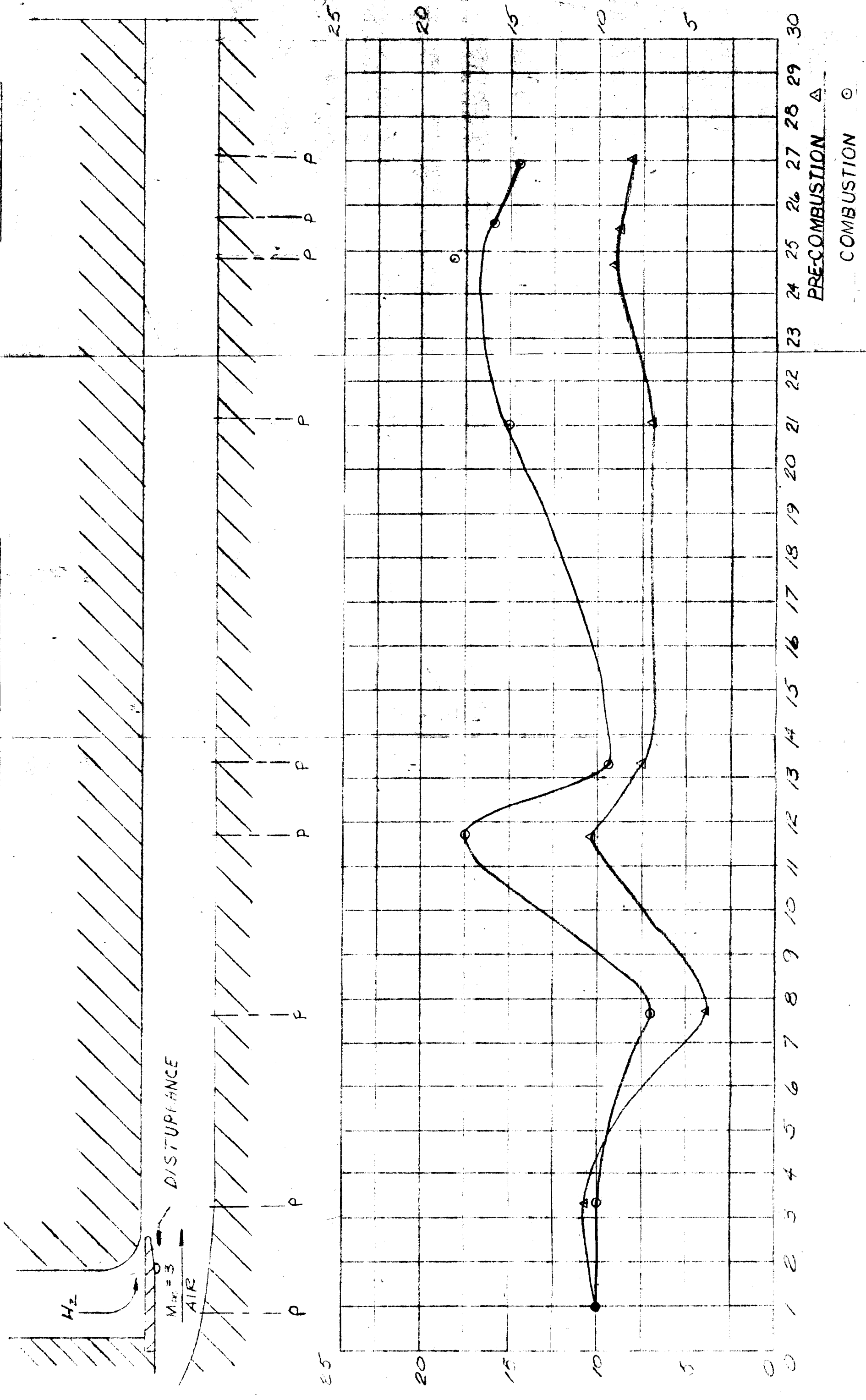
PRESSURE DISTRIBUTION
IN SUPERSONIC JET TUNNEL
RUN NO. 94

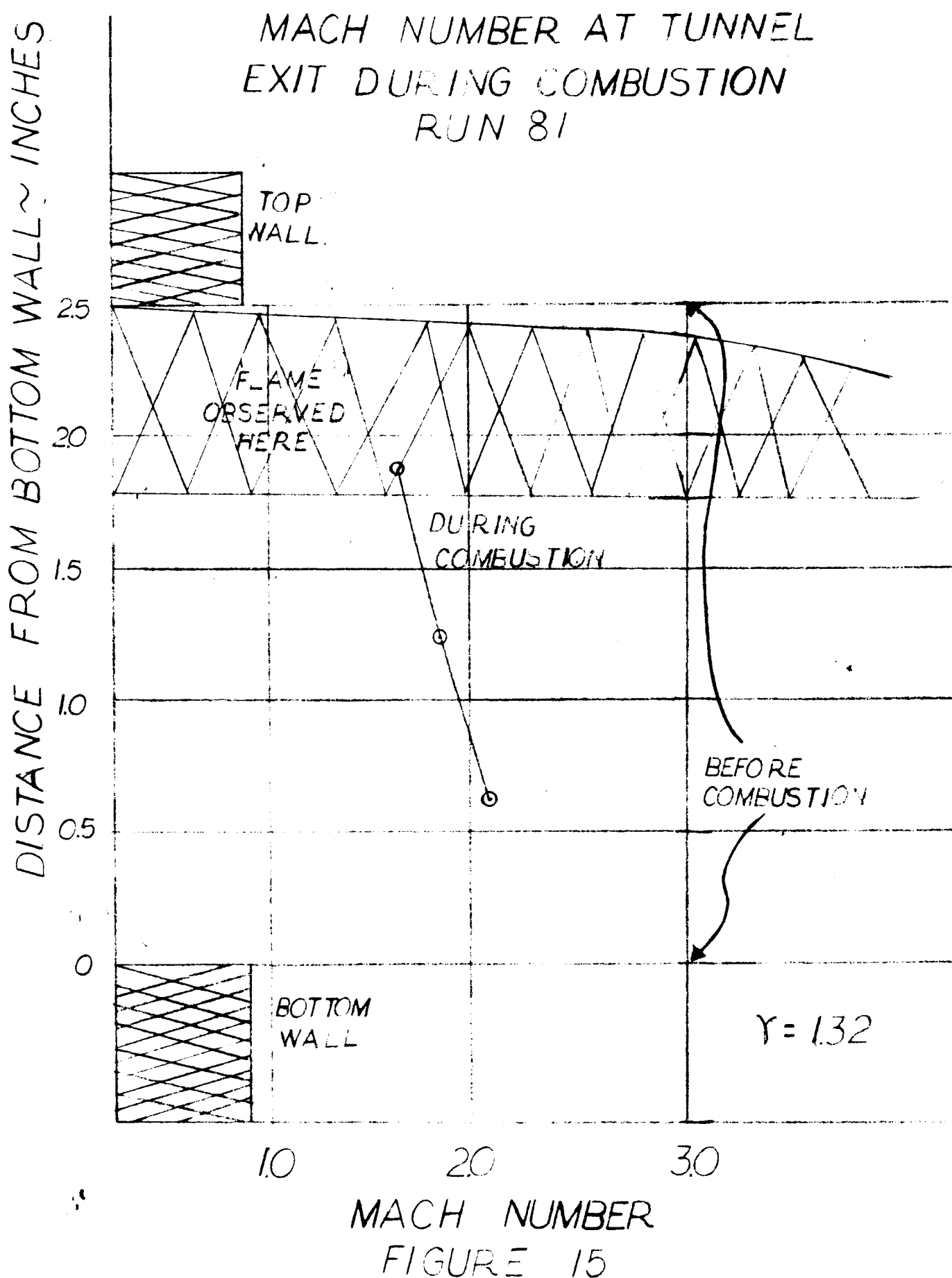
FIGURE 14



PRESSURE DISTRIBUTION
IN SUPER SONIC WIND TUNNEL
BOTTOM WALL
RUN NO. 24

FIGURE 14A





STAGNATION TEMPERATURE PROFILE IN TEST SECTION

DISTANCE FROM BOTTOM WALL, INCHES

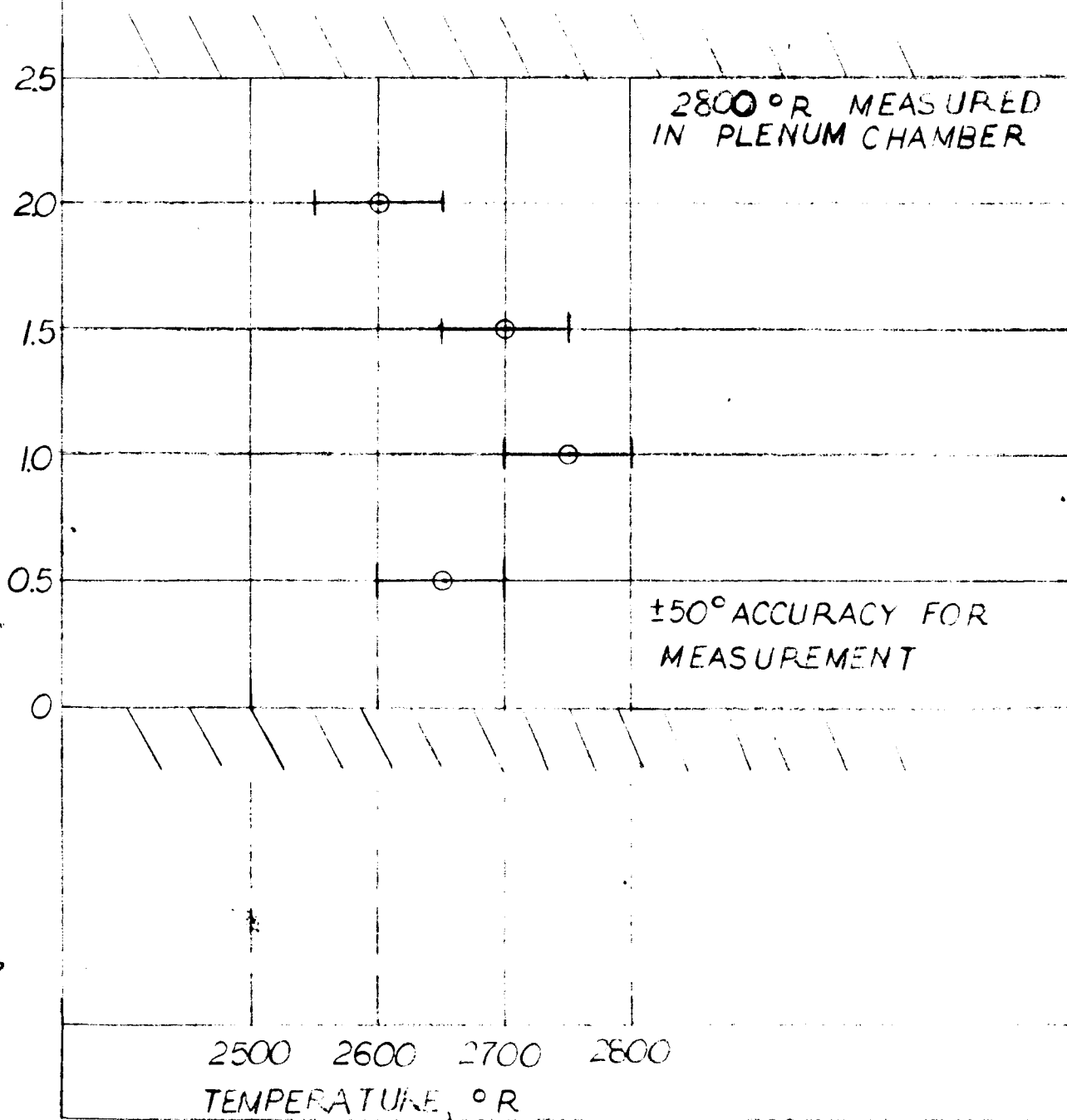


FIGURE 16

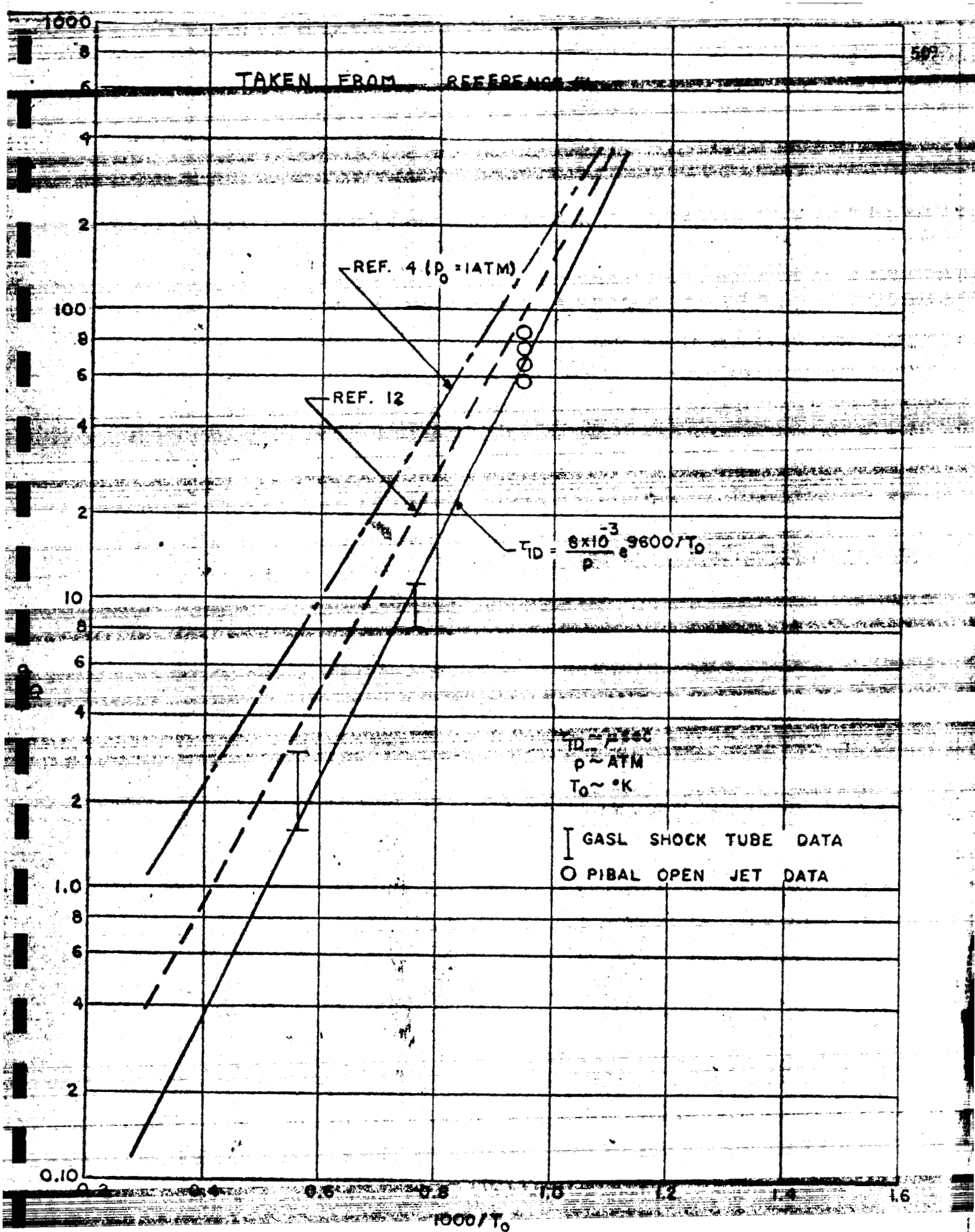


FIG.17 CORRELATION OF IGNITION DELAY TIME NUMERICAL RESULTS

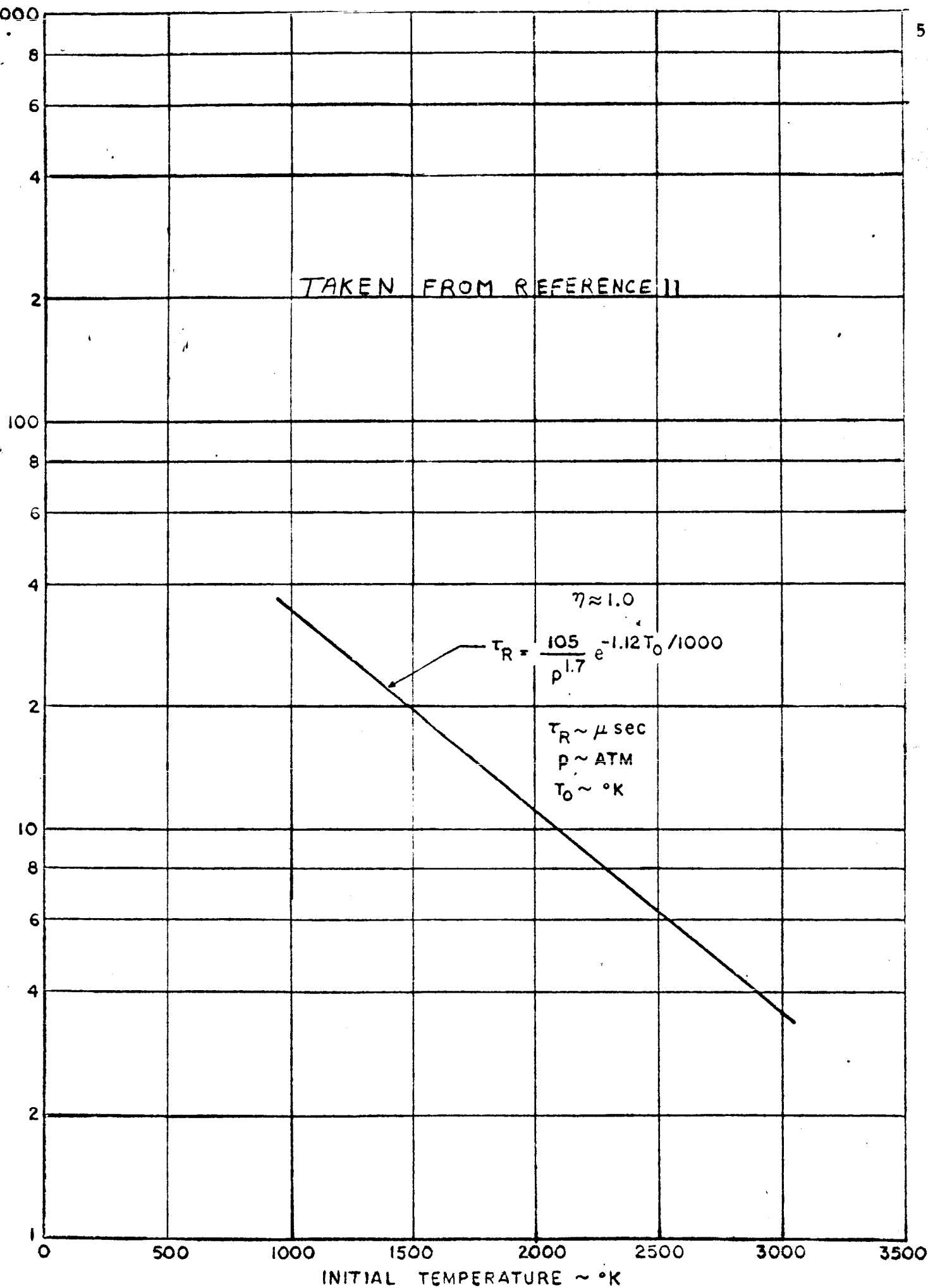


FIG. 18 CORRELATION OF REACTION TIME NUMERICAL RESULTS

TYPICAL LAUNCH VEHICLE TRAJECTORY

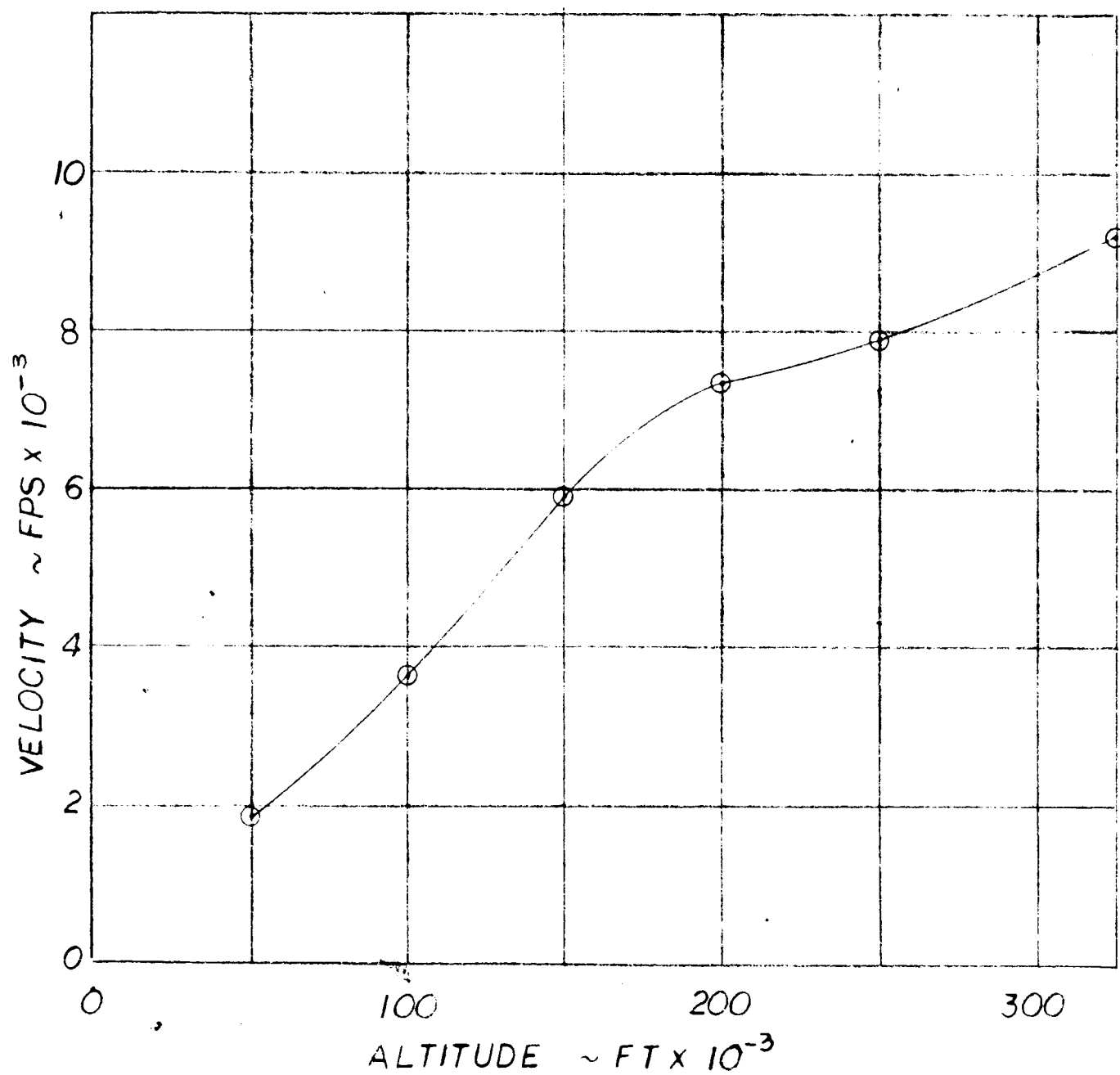


FIGURE 19

MAXIMUM SPLITTER PLATE BOUNDARY LAYER TEMPERATURE ~ °R

ALTITUDE FOR THERMAL IGNITION OF HYDROGEN DUMPED FROM A WALL SLOT

BASED ON: $T_w = 400^\circ\text{F}$

$X = 10\text{ ft}$

$D = 3\text{ ft}$

AND ISENTROPIC EXPANSION
FROM NORMAL SHOCK

$$TO \quad P_e = P_\infty \left(0.44 + 0.08 \frac{X}{D} M_\infty^2 \sqrt{C_D} \right)$$

7000

6000

5000

4000

3000

2000

1000

PROBABLE IGNITION

NO IGNITION

TURBULENT
BOUNDARY
LAYER

LAMINAR
BOUNDARY
LAYER

$Re_{trip} = 10^5$

ALT	Re	P _e
$\frac{\text{ft}}{1000}$	$\times 10^{-5}$	psf
100	10	40
150	2.5	8
200	0.14	3
250	0.06	.05

0

100

200

300

ALTITUDE ~ FT $\times 10^{-3}$

FIGURE 20